Human-induced loading and dynamic response of footbridges in the vertical direction due to restricted pedestrian traffic

A non-intrusive nuclear data uncertainty propagation study for the ARC fusion reactor design

Alex Aimetta,[*,a] Nicolò Abrate,[a] Sandra Dulla,[a] and Antonio Froio[a]

[a] *Politecnico di Torino, Dipartimento Energia, NEMO group*
Corso Duca degli Abruzzi, 24 - 10129 Torino (Italy)

[*]Email: alex.aimetta@polito.it

Number of pages: 48
Number of tables: 18
Number of figures: 18

A non-intrusive nuclear data uncertainty propagation study for the ARC fusion reactor design

Alex Aimetta, Nicolò Abrate, Sandra Dulla, and Antonio Froio

Abstract

It is widely recognized that the safe and robust design of a nuclear system requires an uncertainty propagation (UP) analysis concerning the various nuclear data used as input parameters, especially in view of the most recent design methodologies like the Best Estimate Plus Uncertainty approach. The evaluation of the input uncertainties and their propagation to the design parameters of interest is particularly important in the case of nuclear fusion machines such as the Affordable Robust Compact (ARC) reactor, which is featured by the presence of uncommon isotopes in the nuclear engineering field, like fluorine, beryllium and lithium. The uncertainties on the nuclear data of these nuclides can have a significant impact on fundamental design parameters, such as the target Tritium Breeding Ratio (TBR). Hence, in this work we investigate the application of different methods for propagating the nuclear data uncertainty to the parameters of interest, computed with the Serpent 2 Monte Carlo code. All the methods proposed in this work share the feature of being non-intrusive, implying that they can be profitably employed independently on the physical and/or computational model adopted.

The methods discussed in this work are the fast Total Monte Carlo, the GRS, the Unscented Transform and the Polynomial Chaos Expansion. The first three methods lead to similar values in terms of relative standard deviation on the TBR due to nuclear data, and can be considered as fast alternatives to brute-force sampling methods. For these three methods, the present paper suggests how to select the best approach according to the kind of analysis to be performed and to the nuclides considered in the study. The effect of the use of different nuclear data libraries and of different input covariance matrices is also examined. The main outcome of these analyses suggests that the uncertainties in nuclear data of nickel, fluorine, beryllium and lithium are sufficiently small (i.e. smaller than 1%) to prevent the TBR to assume values below the design constraints. The overall uncertainty on the TBR of ARC due to the nuclides here considered was evaluated

to be $\sim 0.9\%$. Concerning the Polynomial Chaos Expansion approach, the paper shows that its application is computationally inefficient compared to the other techniques when the input data dimensionality is very large, as for the case of nuclear data.

Keywords Uncertainty Propagation, Fast Total Monte Carlo, GRS, Unscented Transform, Polynomial Chaos Expansion

I. INTRODUCTION

The Affordable Robust Compact (ARC) reactor conceptual design,[1] proposed by the Massachusetts Institute of Technology (see fig. 1), is a small -Tritium (D-T) based tokamak with the aim of producing electric power (200 MWe) and with a significant size reduction with respect to other next-generation machines, such as DEMO (DEMOnstration Power Plant).[2] In the ARC design the size minimisation and, as a consequence, its cost and complexity reduction, will be achieved by increasing the magnetic field intensity, thanks to high-temperature superconductors.

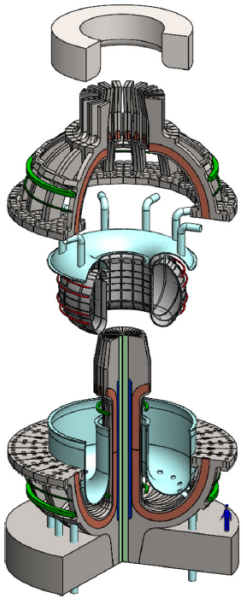

Fig. 1. ARC assembling scheme, reproduced from.[1] Some characteristic dimensions of ARC: plasma major radius 3.3 m, plasma minor radius 1.1 m.

In the current design of ARC, the vacuum vessel is submerged in a breeding blanket filled with a molten salt, i.e. FLiBe (76.79% fluorine, 9.09% beryllium and 14.12% lithium). The FLiBe salt works simultaneously as neutron multiplier, neutron moderator, radiation shield, heat transfer fluid, tritium breeder, and tritium carrier, and it is continuously circulating. In order to achieve a Tritium Breeding Ratio (TBR) larger than one, thus ensuring the reactor self-sustainability and a closed fuel cycle, the lithium in the salt is isotopically enriched in ^{6}Li up to 90%. In this reactor, the neutron multiplier used to enhance the overall neutron economy is beryllium, present both in the molten salt composition and in a layer inside the vacuum vessel.

The preliminary neutronic modelling of ARC has been performed with the Monte Carlo particle transport code Serpent 2 (v. 2.1.31)[3] in a previous work,[4] for the evaluation of the tritium breeding ratio and the power deposition by neutrons and photons inside the breeding blanket, proving the capability of Serpent to suitably simulate fusion reactors, leading to an estimated TBR>1, using the ENDF-B/VIII.0 nuclear data library. The scripts employed to develop the Serpent model of ARC are available in a Zenodo repository.[5] In this work, the same ARC reactor model, sketched in fig. 2, is used with a focus on the nuclear data uncertainty quantification and propagation.

The most popular approach to evaluate the uncertainty, when the number of uncertain input and output parameters is large, is the adoption of perturbation methods. More specifically, concerning the nuclear data uncertainty, the so-called *sandwich rule* is commonly applied:[6]

$$\mathrm{var}[r] = \vec{S}_p^{\,r}\,\mathrm{cov}[p]\,\vec{S}_p^{\,r^T}\,, \tag{1}$$

where $\mathrm{var}[r]$ is the variance of the response, $\vec{S}_p^{\,r}$ is the relative sensitivity of r with respect to a variation in the input p, and $\mathrm{cov}[p]$ is the relative covariance matrix associated with p. The calculation of the relative sensitivity is usually performed using the Generalised Perturbation Theory (GPT).[7] Both this approach and the eXtended Generalised Perturbation Theory (XGPT), which is a continuous-energy extensions of GPT tailored for Monte Carlo transport calculations, are currently available in Serpent 2.[8] Despite both approaches have been satisfactorily applied to criticality calculations in fast fission reactors,[9,10] their implementation does not currently support fixed-source calculations in a non-fissile system, such as the case of the ARC blanket.

The most popular alternative approach to perturbation-based methods is the brute-force sampling, which is known in the field of nuclear data uncertainty quantification and propagation as Total Monte Carlo (TMC).[11] This method is very powerful because it allows to get very rich information about the output uncertainty, namely the full sample distributions of the output responses, without any *ad hoc* implementation in the code, as it would be required for the GPT and XGPT methods. However, these nice features come at the price of a very slow statistical convergence, which scales as $1/\sqrt{N_{exec}}$, where N_{exec} represents the number of model executions.

Most of the times, especially when only a rough value of the uncertainty is needed, as in the case of design calculations, the detailed information provided by TMC is not worth its com-

putational cost. This is certainly the case of ARC: considering that a robust design requires the evaluation of the uncertainty induced by different isotopes, the TMC would not be a computationally affordable approach.

A good compromise between the good computational performances of perturbation methods and the non-intrusiveness of TMC can be found applying other sampling-based, non-intrusive uncertainty propagation (UP) methods, which allow to reconstruct the lower-order moments of a distribution in a computationally efficient manner. More specifically, this paper will present four methods, namely the fast Total Monte Carlo,[12] the GRS,[13] the Unscented Transform[14] and the Polynomial Chaos Expansion.[15] The first two approaches, which are quite similar, are tailored for the uncertainty propagation through a stochastic model, like the Serpent 2 ARC model, whilst the last two methods can be applied to deterministic models as well and allow to achieve good computational performances by a smart sampling of the input parameter space. Examples of alternative stochastic perturbation based techniques[16,17,18] and of deterministic approaches[19,20] successfully applied to fusion systems can be found in the literature.

The aim of the paper is to provide an overview of these methods, applying them to carry out the nuclear data uncertainty propagation for some selected responses of interest, namely the TBR and the power deposited by the nuclear reactions in the various components of the reactor. In this respect, it is mandatory to perform the UP analysis in order to guarantee that TBR>1, even considering the nuclear data uncertainties. In particular, since the power deposition and the TBR are mostly influenced by the nuclides composing the liquid breeding blanket, i.e. ^{6}Li, ^{9}Be and ^{19}F, this study will deal mainly with these isotopes.

The paper is organised as follows: in section II the impact of the different nuclear data library selection on the nominal response quantities is evaluated; in section III the main algorithms for the uncertainty propagation are described, focusing on their peculiarities for this specific application; in section IV the results of the application of the methods are presented and discussed; in section V some concluding remarks, useful for future nuclear data uncertainty propagation studies, are drawn, and some future perspectives are given, together with two tables that sum up the main results of this work for what concerns the TBR and the total neutron power deposition in ARC.

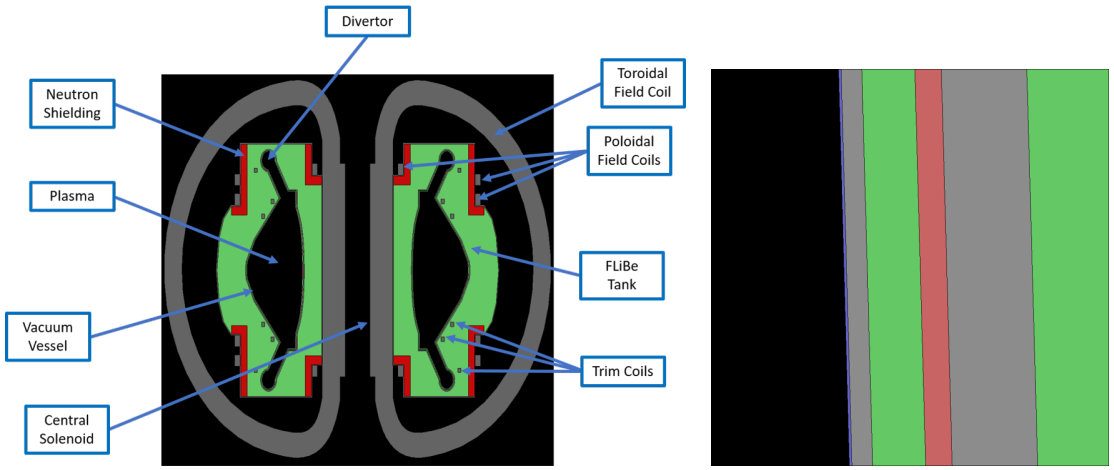

(a) (b)

Fig. 2. Poloidal section of the ARC model implemented in Serpent (a), and detail of the radial build of the vacuum vessel (b). From the left to the right: plasma chamber (black), first wall (blue), inner vacuum vessel (gray), cooling channel (green), neutron multiplier (red), outer vacuum vessel (gray) and FLiBe blanket (green).

II. NOMINAL SIMULATIONS WITH DIFFERENT NUCLEAR DATA LIBRARIES

One of the most recent methodologies for the safety assessment and for the design verification of nuclear systems is the so-called Best Estimate Plus Uncertainty (BEPU) approach,[21,22] which qualifies the output computed by best estimate computational codes providing an estimate of their uncertainty. Compared to other branches of nuclear engineering, e.g., thermal-hydraulics and thermal-mechanics, neutronics is characterised by two peculiarities. The first one is that, within a certain statistical tolerance, the Monte Carlo approach potentially allows to obtain an *exact* solution to the neutron transport equation, since no approximation is introduced in the reactor geometry and both the energy and the flying directions of neutrons are sampled continuously. Hence, being a discretisation-free method, the Monte Carlo approach could be considered the reference best estimate tool available for neutronic analyses. The second peculiarity of neutronics is that, independently on the approach used to solve the neutron transport equation, the model requires as input a set of complex experimental data regarding, essentially, the interaction between neutrons and matter. Thus, it should be clear that an additional source of uncertainty, beyond the statistical one induced by the Monte Carlo method, is due to the input nuclear data. In this respect, the BEPU approach applied to the neutronic design of a nuclear fission or fusion reactor

means that the best estimate values produced with Monte Carlo calculations should be provided with their uncertainties.

Since there are different nuclear data evaluations available in the literature, assessing the impact of the nuclear data library selection on the best estimate output values is of paramount importance for both the reactor design and its safety demonstration. This section aims at showing the impact of the nuclear data library choice on the main macroscopic parameters of interest for the ARC design, namely the TBR and the power deposition in various regions of the reactor.

Because of the huge range of the incident neutron energy and of the great variety of reaction channels featuring the various isotopes composing the reactor media, the nuclear data are stored in a specific file format, known as Evaluated Nuclear Data Files (ENDF). The ENDF format cannot be read as it is by Serpent, which requires the nuclear data to be processed as ACE (A Compact ENDF) files. The conversion of the ENDF files into the ACE format is usually performed using suitable nuclear data processing tools; among the various codes available to perform this task, NJOY is certainly the most popular and reliable one.[23] To ensure the full consistency in the ENDF-to-ACE conversion process for the different libraries selected for the calculations, namely ENDF-B/VIII.0, JEFF-3.3 (Joint Evaluated Fission and Fusion), the beta version of JEFF-4 and FENDL-3.2b (Fusion Evaluated Nuclear Data Library), an in-house, open-source Python class have been conceived to manage automatically and efficiently the file processing with NJOY, guaranteeing that the same processing settings are adopted for the various libraries and, thus, that the differences obtained in the best estimate calculations are only due to the nuclear data evaluations.

In a previous work,[4] some Serpent simulations for the evaluation of the TBR and the power deposition were performed using the ENDF-B/VIII.0 library. For this reason, in the present work, this library is considered as the reference one. For the other libraries, a series of Serpent simulations with the same setup are performed, modifying only the nuclear data library selection. Each neutronic simulation is run using 10^8 neutron histories, subdivided into 100 batches, in order to guarantee that the relative differences of the responses of interest between different libraries is larger than their statistical uncertainty.

The bars in fig. 3 are useful to visualise the differences between the nuclear data libraries. At first, it is possible to observe their impact on the value of the TBR. The lowest value is obtained with FENDL-3.2b, while the largest one is obtained using ENDF-B/VIII.0. At a first glance, the

variation could appear small, but it is important to underline that even an extremely small change in the value of the TBR obtained with the neutronic simulation (the so-called global TBR) can lead to a target TBR (i.e. the TBR which takes into account all the tritium losses in the fuel cycle, inaccuracies in the geometry model and nuclear data uncertainties[24]) smaller than one.

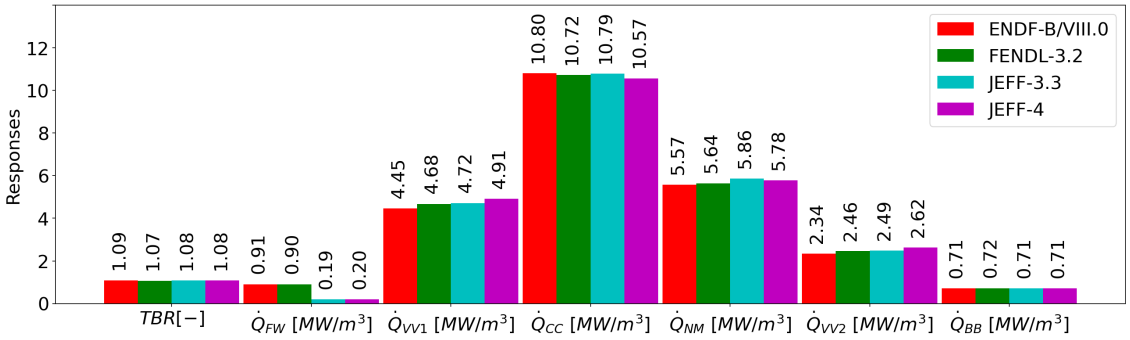

Fig. 3. Comparison of different nuclear data libraries in the evaluation of the TBR, the average volumetric power deposition in the first wall ($\dot{Q}_{FW}$), the average volumetric power deposition in the inner vacuum vessel ($\dot{Q}_{VV1}$), the average volumetric power deposition in cooling channel ($\dot{Q}_{CC}$), the average volumetric power deposition in the outer vacuum vessel ($\dot{Q}_{VV2}$) and the average volumetric power deposition in the breeding blanket ($\dot{Q}_{BB}$). The error bars are not visible because the statistical uncertainty is too small.

Another significant discrepancy concerns the volumetric power deposition in the tungsten-made first wall, where the value obtained with the JEFF libraries is significantly smaller than the others. This is due to the fact that the JEFF libraries miss some KERMA values in the high energy range, which plays a significant role in this case since the first wall is directly in contact with the neutron plasma source at 14.1 MeV, see fig. 4. On the other hand, the power deposition in the first wall obtained with the ENDF-B/VIII.0 and the FENDL-3.2 libraries are similar because the KERMA values of tungsten at high energy in the two libraries are the same.

In the case of both vacuum vessels, there is a non-negligible increase of the power deposition computed with the other libraries with respect to the reference one, i.e. ENDF-B/VIII.0. One of the causes is probably the fact that the KERMA values of ^{58}Ni, which is the most abundant isotope in the vacuum vessel, are smaller in the ENDF-B/VIII.0 library, particularly in the lower energy range ($E < 0.01$ MeV), see fig. 5.

Finally, in order to have a more intuitive representation of this comparison, fig. 6 displays the ratio between the radial power deposition using FENDL-3.2b, JEFF-3.3 and JEFF-4 with respect to the ENDF-B/VIII.0 case, for the various layers that separate the plasma and the breeding

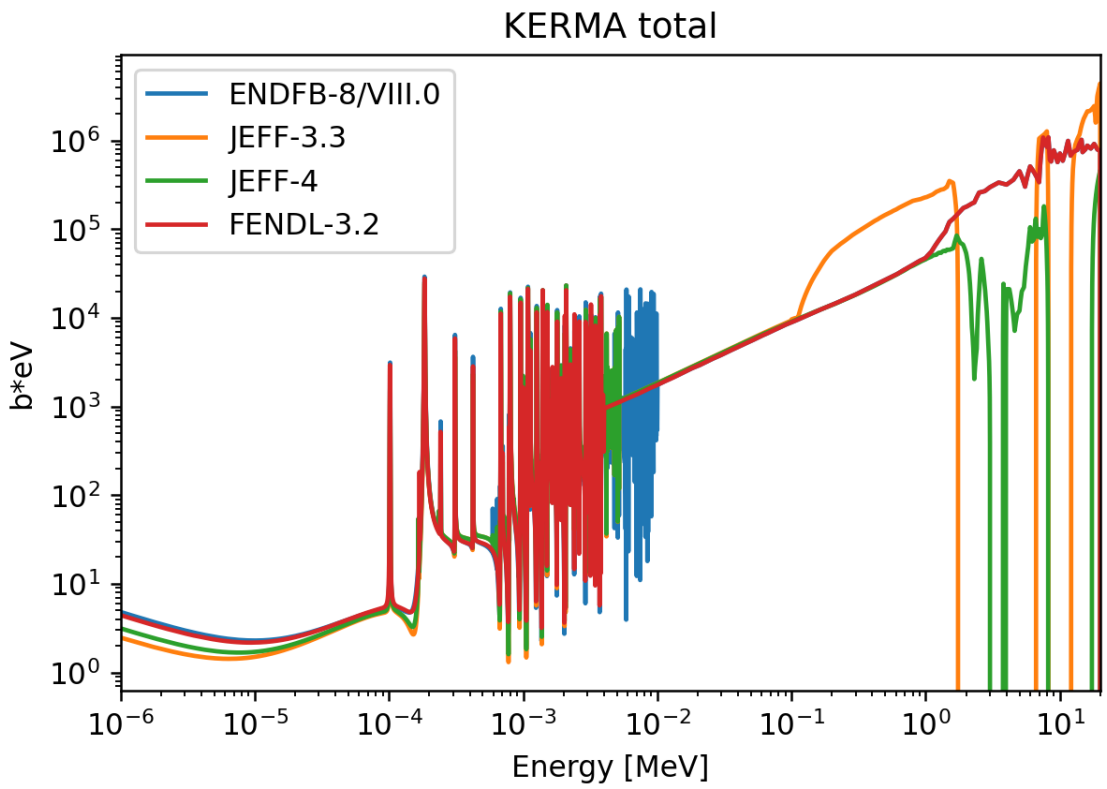

Fig. 4. KERMA coefficients (MT=301) of ^{184}W for the different nuclear data libraries considered in this work.

blanket at the mid-plane of ARC. Again, the largest differences can be appreciated in the inner and the outer vacuum vessels.

III. UNCERTAINTY PROPAGATION METHODS

In this section, the uncertainty propagation (UP) methods employed in the present work are briefly described. As mentioned, the choice of non-intrusive methods requires no need for modifications of the original model, but only the generation of a set of perturbed nuclear data to be employed in a set of neutronic Monte Carlo simulations.

The tool used for the generation of the perturbed data for this analysis is the SANDY Python package,[25] which has been selected since it is open-source, user-friendly and well integrated with the nuclear data processing code NJOY. SANDY requires only the first two moments of the data distributions, namely their expected values and their covariances, thus it is assumed that the

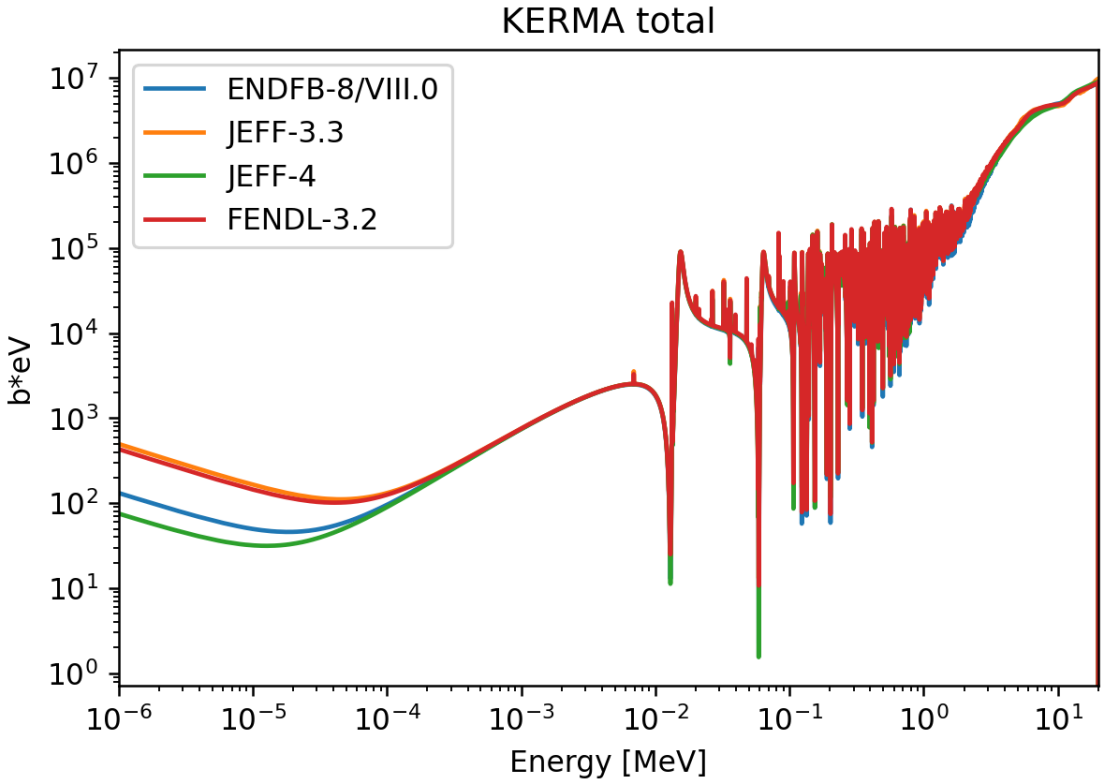

Fig. 5. KERMA coefficients (MT=301) of ^{58}Ni for the different nuclear data libraries considered in this work.

perturbed data are normally distributed. At the time the calculations were performed, SANDY allowed only to sample the data perturbation according to a Gaussian distributions, meaning that negative cross sections could arise from the sampling process. To solve this inconsistency in the dataSANDY enforces the perturbation coefficients falling outside the range $[0, 2]$ to 0 or 2 if they are lower than 0 or larger than 2, respectively. It is worthwhile mentioning that the most recent versions of SANDY have the capability of performing samplings based on log-normal distributions to avoid negative values.

Initially, all the nuclear data and the corresponding covariances used for the analysis are taken from the ENDF-B/VIII.0 library. This choice was made to be consistent with the Serpent simulations presented in,[4] performed using this library. However, considering that the covariance data depend on the data library evaluation, also the impact induced by the choice of other libraries is taken into account, performing calculation using FENDL-3.2b and JEFF-3.3. The JEFF-4

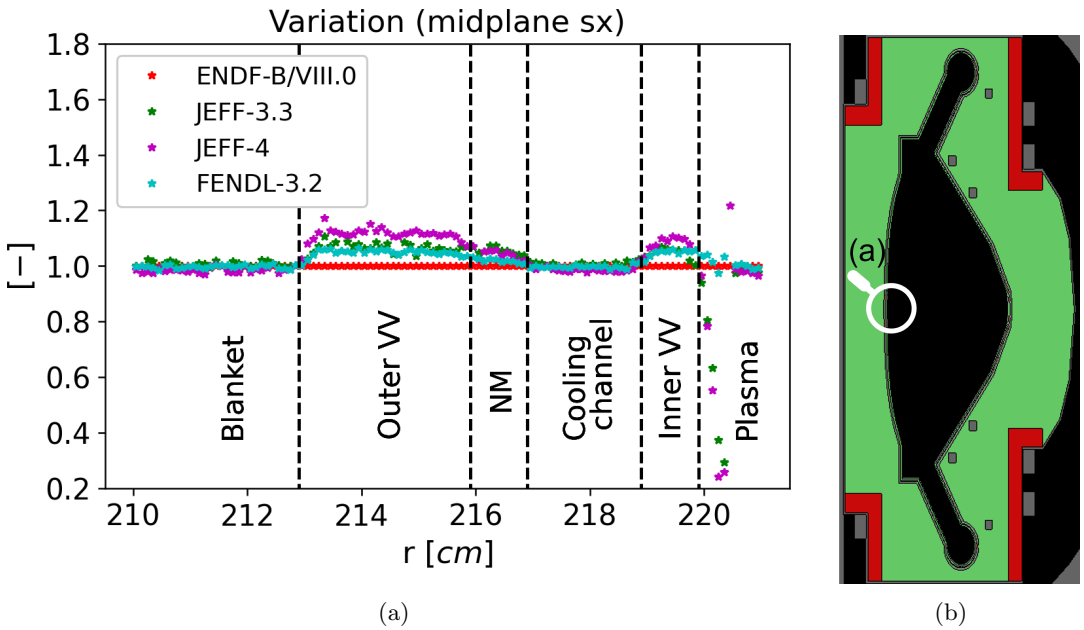

(a) (b)

Fig. 6. (a) Ratio of the radial power deposition in the inboard side of the equatorial region obtained using FENDL-3.2b, JEFF-3.3 and JEFF-4 with respect to ENDF-B/VIII.0 and (b) position of the detectors employed for the evaluation.

library has not been considered because it misses information about the covariance matrices of the most important reaction channels of the ^{9}Be, i.e. elastic scattering and neutronic multiplication, and it does not contain any covariance matrices of the ^{19}F. In this work, the data covariances for the resonance parameters (MF=33) and for the reaction cross sections (MF=34) have been considered, thus generating physically consistent perturbed ACE files.

III.A. Fast Total Monte Carlo

The fast Total Monte Carlo (fTMC) method[12] is a faster alternative to the reference Total Monte Carlo method.[11] The fTMC performs roughly the same number of Monte Carlo simulations of TMC, but each one with a reduced number of neutron histories, using a different seed for the random number generator and a different perturbed nuclear data library. The adoption of a reduced number of neutron histories allows to fairly reduce the computational time, at the price of a poorer statistical information, since only the second order moment can be estimated by exploiting

the definition of the total variance,

$$\sigma^2_{ND} = \sigma^2_{obv} - \overline{\sigma}^2_{stat}, \tag{2}$$

where σ^2_{ND} is the *epistemic* uncertainty due to the nuclear data, $\overline{\sigma}^2_{stat}$ is the average of the statistical variances of the simulations, i.e. the *aleatoric* variance, while σ^2_{obv} is the total variance of the vector of observables.

Looking at eq. (2) it is clear that when the statistical variance is too large, the variance induced by the nuclear data may turn out to be negative. This inconsistency with the variance definition is due to the fact that the statistical noise actually covers the one induced by the nuclear data. To avoid this situation, the total number of particle histories should be selected to yield a sufficiently low statistical noise.

At the end of the fast Total Monte Carlo simulations, the resulting responses are cast as a vector of observables (e.g, a vector of TBR values) and a vector of statistical errors, that can be used in eq. (2) to estimate the epistemic uncertainty due to the nuclear data. With respect to the TMC application, the computational time is reduced by a factor of nN_{exec}, where n is the ratio between the neutron histories between TMC and fTMC and N_{exec} is the number of model executions.

III.B. GRS Method

Another fast alternative to the TMC is the GRS method,[13] which requires two different set of simulations, each simulation featured by a different perturbed nuclear data library and a number of neutron histories n times smaller than the TMC. The simulations belonging to each of the two sets share the same seed for the initialisation of the random number generator. The adoption of the same seed for each set guarantees that the only variation in the output response of each set is due to the nuclear data epistemic uncertainty. In such a way, the ensemble of the model responses belonging to each set, namely $\vec{v}_1$ and $\vec{v}_2$, turns out to be statistically independent but identically distributed. Thus, the following expression holds,

$$\sigma^2_{ND} = \mathrm{var}(\mathrm{E}(v_1|\vec{D})) = \mathrm{cov}(\vec{v_1}, \vec{v_2}), \tag{3}$$

that is, the covariance of the two vectors of observables is equal to the variance of the conditional expectation of v_1 given the input data $\vec{D}$, which is the source of the epistemic uncertainty.

Similarly to the fTMC approach, the GRS method is characterised by a fair reduction of the usual computational time of TMC, which amounts in this case to a factor of $\frac{n}{2}N_{exec}$. The larger computational time of GRS compared to fTMC is compensated by the fact that the first approach always provides a positive value for the response variance. Thus, the GRS method is less sensitive than fTMC to the impact of the statistical noise and, consequently, to the number of neutron histories used to carry out the Monte Carlo calculations. In this respect, the user should only guarantee that the inactive histories are sufficient to yield a physically significant fission source,[26] in the case of criticality calculations, or external source (as in our case) convergence: if the number of histories was too low, the emitted particles may not follow the source definition.

III.C. Unscented Transform

The Unscented Transform (UT)[14] is based on the intuition that, to estimate the first and second order moments of the response distribution, it is better to approximate the input distribution rather than approximate the model used to generate the output distribution, especially when the model is non-linear. The input approximation is realised generating a set of sigma points that represent the probability distribution of the input data, independently on its nature. Usually, $2k+1$ sigma points are sufficient to get a good representation of the input, where k represents the dimensions of the input perturbed data. In this case, k is equal to $n_{MT}H$, where n_{MT} is the number of different MT reaction channels in the ENDF file of the nuclide under examination, whereas H represents the number of energy groups employed to extract the covariance matrix. The usual way to overcome this issue consists in the adoption of a suitable reduction technique, which will be described in the following.

Given the covariance matrix $\hat{C}$ of the input, the components of the sigma points vector $\vec{\chi}$ are computed according to the following definitions:[27]

$$\begin{aligned} \chi^{[0]} &= \mu \\ \chi^{[i]} &= \mu + \left(\sqrt{(k+\lambda)\hat{C}}\right)_i \quad \text{for } i = 1, ..., k \\ \chi^{[i]} &= \mu - \left(\sqrt{(k+\lambda)\hat{C}}\right)_{i-n} \quad \text{for } i = k+1, ..., 2k, \end{aligned} \tag{4}$$

where μ is the mean vector of the input (in our case, the mean nominal cross sections from the nuclear data library), λ is an arbitrary spreading parameter that has to be carefully chosen in the case of Monte Carlo simulations (see section IV.B for more details), and $\hat{C}$ is the corresponding covariance matrix. Once the sigma points have been obtained, each one of them is assigned a weight, calculated as follows:

$$\begin{aligned} \omega^{[0]} &= \frac{\lambda}{k+\lambda} \\ \omega^{[i]} &= \frac{1}{2(k+\lambda)} \quad \text{for } i = 1, ..., 2k. \end{aligned} \tag{5}$$

The sigma points are generated so that their mean and covariance is calculated as:

$$\mu = \sum_{i=0}^{2k} \omega^{[i]} \chi^{[i]}, \tag{6}$$

$$\hat{C} = \sum_{i=0}^{2k} \omega^{[i]} \left(\chi^{[i]} - \mu\right) \left(\chi^{[i]} - \mu\right)^T. \tag{7}$$

Finally, the sigma points are passed as an input to the non-linear function $\mathcal{M}'$ (i.e the Serpent simulations in this case) and the weighted mean and weighted covariance of the transformed distribution are calculated as:

$$\mu' = \sum_{i=0}^{2k} \omega^{[i]} \mathcal{M}'\left(\chi^{[i]}\right), \tag{8}$$

$$\hat{C}' = \sum_{i=0}^{2k} \omega^{[i]} \left(\mathcal{M}'\left(\chi^{[i]}\right) - \mu'\right) \left(\mathcal{M}'\left(\chi^{[i]}\right) - \mu'\right)^T, \tag{9}$$

where the index i represents the *i-th* sigma point and weight. The value of $\hat{C}'$ represents the uncertainty on the output results of the model, obtained propagating the nuclear data uncertainties through the neutronic model itself.

The definition of the sigma points and of the weights depend on an arbitrary parameter λ, which represents the spreading of the sigma points. Since the input is assumed to follow a multivariate Gaussian distribution, the best choice according to the literature seems to be $k + \lambda = 3$.[14] However, in case k is large, as in this case, this choice could lead to a set of negative weights $\omega^{[i]}$. This is not an issue for deterministic models, but it could jeopardise the UT approach in case a stochastic model is employed, as it is discussed more in detail later.

As mentioned above, the main drawback of this method is the computation of the square root of the perturbed data input covariance matrix, necessary to calculate the sigma points. In the case of a symmetric and positive semi-definite covariance matrix, this problem can be handled with the Singular Value Decomposition (SVD),[27]

$$\hat{C} = V\Sigma V^T, \tag{10}$$

where the matrix Σ is a diagonal matrix composed by the singular values of $\hat{C}$. When $\hat{C}$ is positive semi-definite, its square root can be computed as:

$$\sqrt{\hat{C}} = V\Sigma^{1/2}. \tag{11}$$

However, it is likely that, because of some round-off errors occurring in the extraction process of the multi-group covariance from the nuclear data libraries, the matrix extracted may be non-positive semi-definite. Thus, before applying the UT, the *statsmodels* Python package[28] is used to evaluate the closest semi-positive definite matrix to the original one, following the procedure given in.[29]

At this point, it is possible to maintain a satisfactory accuracy in the computation of $\hat{C}$ by reducing the number of active singular values obtained with the SVD, thanks to the strong correlation among the nuclear data reactions. As a consequence, the final number of active singular values t is smaller than the number of non-zero singular values r. The k-dimensional covariance matrix that is obtained in this way is thus an approximation of the actual one, and the truncation coefficient t is evaluated computing the so called energy of the singular values:

$$E_t = \frac{\sum_{l=1}^{t} \sigma_i^2}{\sum_{l=1}^{r} \sigma_i^2}, \tag{12}$$

where σ_l^2 is the l-th singular value. This truncation allows to decrease the number of sample points from $2k+1$ to $2t+1$ and the computational time of the uncertainty propagation. In fig. 7, a sketch of the SVD-UT algorithm followed in the paper is provided.

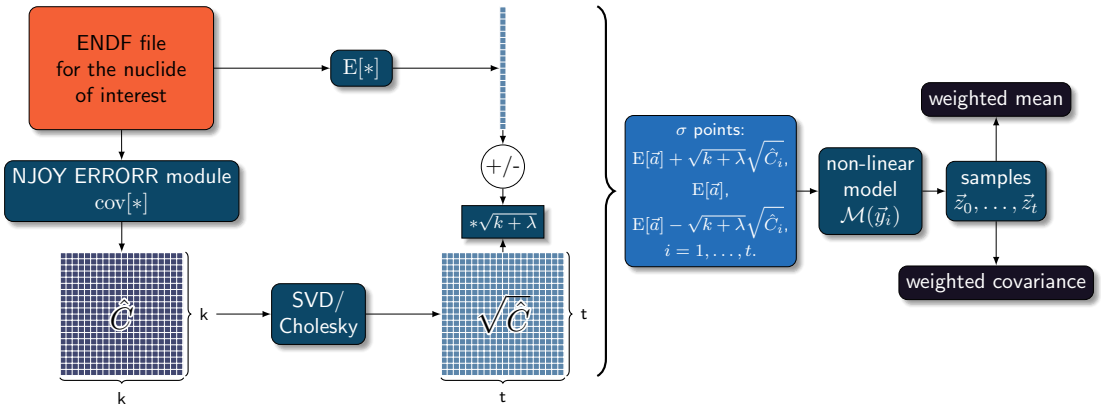

Fig. 7. Schematic of the Unscented Transform method.

III.D. Polynomial Chaos Expansion

The Polynomial Chaos Expansion (PCE) is a very popular technique for uncertainty propagation and sensitivity analysis that was first suggested in[30] and then extended and rigorously formalised in.[31]

The basic idea of the PCE approach, which belongs to the class of spectral methods,[32] is to express a stochastic model $\mathcal{M}$ in terms of an expansion of orthogonal polynomials Ψ,

$$\mathcal{M}(\vec{s},t,\vec{p}) = \vec{y} = \sum_{k=0}^{\infty} \vec{a}_k(\vec{s},t)\Psi_k(\vec{p}) \approx \sum_{k=0}^{K} \vec{a}_k(\vec{s},t)\Psi_k(\vec{p}), \tag{13}$$

where $\vec{s}$ is the vector of the state variables (e.g., spatial coordinates and energy), t is the time, $\vec{p}$ is the vector of stochastic parameters (in this case, the energy dependent cross sections) and $\vec{a_k}$ is the k-th expansion coefficient, which is obtained by means of a projection, weighted on the random variable distribution $w(\vec{p})$, of the model on the k-th basis function, namely

$$\vec{a}_k(\vec{s},t) = \int_{-\infty}^{+\infty} d\vec{p}\mathcal{M}(\vec{s},t,\vec{p})\Psi_k(\vec{p})w(\vec{p}). \tag{14}$$

The choice of the orthogonal polynomial basis is determined by the distribution of the random variables.

If the vector of random input parameters was constituted by independent random variables,

the multivariate polynomial basis would be defined as

$$\Psi_k(\vec{p}) = \prod_{i=1}^{d} \psi_i(p_i), \tag{15}$$

where d is the number of independent random variables.

The calculation of the projection coefficients, whose number depends both on the desired polynomial order K and on the number of independent random variable d, can be carried out following different strategies. Concerning non-intrusive procedures, which allow to treat the model $\mathcal{M}$ as a black-box, it is possible to identify two general procedures,[33] namely:

- *the pseudo-spectral approach*, which consists in approximating eq. (14) through a quadrature rule,
$$\vec{a}_k(\vec{s}, t) = \int_{-\infty}^{+\infty} d\vec{p}\mathcal{M}(\vec{s}, t, \vec{p})\Psi_k(\vec{p})w(\vec{p}) \approx \sum_{i=1}^{I} \mathcal{M}(\vec{s}, t, \vec{p}_i)\Psi_k(\vec{p}_i)w(\vec{p}_i); \tag{16}$$
- *the least-square regression approach*, which consists in approximating the PCE coefficients $\vec{a}_k$ through a least-square fit.

One of the advantages of the first approach is that, in many situations, a limited number of points is sufficient to provide a good estimate of eq. (14). For example, in a few dimensional problem, the Gauss quadrature would allow to integrate exactly all the polynomials with a degree $2n-1$ or less with n model evaluations. On the contrary, the accuracy of the regression approach would depend on the choice of the model samples, thus it would be more difficult to assess its adequateness. As expressed in eq. (15), when the input vector $\vec{p} \in \mathbb{R}^d$ is constituted by independent random variables, the multivariate polynomials would be expressed as a product of univariate polynomials, meaning that the number of their coefficients and, thus, the number of integral evaluations, would grow exponentially with the number of dimensions, due to the so-called *curse of dimensionality*.[34] In this respect, the least-square regression could be more convenient than the pseudo-spectral method.

Moreover, since the nuclear data are correlated, they need to be decorrelated using the Kharunen-Loeve transformation (eq. (17)), before employing the PCE:

$$\vec{x} = \vec{\mu} + \sum_{i=1}^{r} \sqrt{\lambda_i}\xi_i\vec{p}_i \tag{17}$$

where $\vec{\mu}$ is the mean nominal cross sections vector from the nuclear data library, $\sqrt{\lambda_i}$ and $\vec{p}_i$ are, respectively, the *i-th* eigenvalue and the *i-th* eigenvector of the nuclear data covariance matrix and ξ represent a set of independent standard normal random variables. Thus, also in this case, it is possible to apply the SVD on the covariance matrix in order to obtain its eigenvalues and eigenvectors and to reduce the number of non-zero eigenvalues r, with the purpose of reducing the dimension of the problem from r to t, as in the UT method. At the end of this procedure, there will be a set of q cross section vectors, which correspond to q Serpent simulations necessary to evaluate the coefficients a_i.

The number q corresponds to the number of points that are used to sample the joint standard normal distribution with reduced dimension t. There are several ways in order to sample the joint distribution. As already mentioned, we have selected two non-intrusive methods available in the Chaospy[35] Python package: the pseudo-spectral and the least-square regression (also known as point collocation) methods.

In the pseudo-spectral approach, quadrature nodes and weights are generated from a quadrature integration scheme (e.g., Gaussian quadrature). Then, these nodes are used to generate a set of q vectors $\vec{x}$ in order to perform q Serpent evaluations. At this point, it is necessary to select a proper order for the expansion of polynomials so that it will be possible to estimate the PCE coefficients through quadrature integration. Finally, information about the distribution of the response can be obtained using eq. (16) as a proxy for the real model. Thus, in the pseudo-spectral method, the number of Serpent simulation is determined by the quadrature integration scheme and cannot be arbitrarily selected.

The alternative is to use the regression method, where the samples are generated either using the quadrature nodes or, more frequently, through random or quasi-random sampling. Similarly to the pseudo-spectral technique, Serpent evaluations are performed using these samples. Then, after having selected an order for the expansion of polynomials, the linear regression problem with respect to the polynomial coefficients is solved in order to construct the model approximation, used to obtain information about the response distribution. In this case, if one uses the random sampling, it is possible to select an arbitrary number of sampling points (i.e. of Serpent simulations). However, obviously, this number can not be too smaller than the number of quadrature points in the pseudo-spectral method, in order to accurately compute the PCE coefficients.

IV. RESULTS

In this section, the most significant results obtained with the different methods are presented. In section IV.A, the fTMC and GRS results are presented together, due to the similarities between these techniques. The results of the UT are then shown in a dedicated section (IV.B), since they require a more in-depth analysis. Some preliminary results with the PCE can be found section IV.C. Finally, some considerations are drawn about the impact on the uncertainty propagation results of the choice of different nuclear data libraries, in section IV.D, and of different group structure, in section IV.E. The perturbed nuclear data files employed for the UP analysis can be found in.[36]

IV.A. Fast Total Monte Carlo and GRS

The first calculations are carried out with the fast Total Monte Carlo approach, because of its better computational performances with respect to the GRS method. For both ^{9}Be and ^{19}F, 500 simulations were carried out, each one with a different perturbed ACE file, generated with SANDY. Each simulation was run using 50 neutron batches, with 10^4 neutron histories per batch, which has been considered a sufficiently high number in order to obtain a statistical uncertainty smaller than the epistemic one. 500 perturbed nuclear data can be considered as a sufficient number too, since the results seem to have reached a good convergence after 500 Serpent simulations (fig. 8 and table I).

TABLE I
Relative standard deviation of the TBR after 500 Serpent simulations performed with the fTMC for the nuclides of interest.

	^{6}Li	^{9}Be	^{19}F	^{58}Ni
RSD [%]	0.0048	0.0143	0.0248	0.0316

In the case of ^{6}Li, the number of neutron histories adopted was not sufficient to obtain a positive nuclear data uncertainty from eq. (2). This was a first indication of the fact that the impact of ^{6}Li on the response uncertainty is not significant. Nevertheless, to confirm this conjecture, the number of neutron histories per batch was increased to 3×10^4 only for this nuclide in order to reduce the statistical error and to obtain a positive nuclear data uncertainty.

The results with the fTMC for the TBR are shown in table II. The contribution of ^{6}Li on the epistemic uncertainty is negligible compared to the statistical one, being one order of

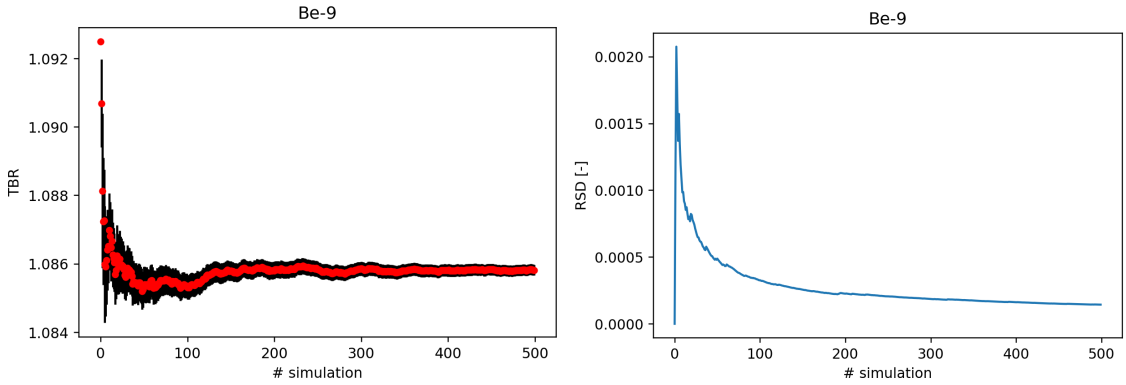

(a) (b)

Fig. 8. (a) Convergence plot of the TBR values resulting from 500 simulations of the fTMC method with ^{9}Be and (b) relative standard deviation. The black lines represent the 1σ error bars.

magnitude smaller than those of the other two nuclides. On the other hand, the relative standard deviations (RSD) for ^{9}Be and ^{19}F due to the nuclear data are larger than the statistical ones and are independent of the number of neutron histories simulated, confirming that they are the epistemic contributions.

TABLE II
Nuclear data uncertainty for the TBR evaluated with the fast Total Monte Carlo method using the ENDF-B/VIII.0 library.

	^{6}Li	^{9}Be	^{19}F
TBR [-]	1.085±0.002	1.086±0.003	1.086±0.006
Statistical RSD [%]	0.1063	0.1829	0.1825
Nuclear data RSD [%]	0.0135	0.2631	0.5245

The same type of analysis has been performed with the GRS method, doubling the computational time (see section III.B above) with respect to the other method, still using 10^4 neutron histories per batch.

Comparing the results of the GRS method in table III with the ones of the fast Total Monte Carlo, it is possible to observe a very good agreement for what concerns ^{9}Be and ^{19}F, suggesting, in this case, that the adoption of the fTMC is preferable due to its lower computational time. On the other hand, regarding ^{6}Li, the GRS has lead to a negative covariance, differently from what explained in section III.B. This is probably due to the fact that the contribution of the perturbations on the ^{6}Li nuclear data are so small that the GRS is not able to give physical

results. Thus, in the case of ^{6}Li, a negative covariance can be read as the fact that the effect of the nuclear uncertainties of ^{6}Li is negligible, as already stated in the case of the fTMC.

TABLE III
Nuclear data uncertainty for the TBR evaluated with the GRS method using the ENDF-B/VIII.0 library.

	^{6}Li	^{9}Be	^{19}F
TBR [-]	1.087±0.001	1.083±0.003	1.086±0.006
Statistical RSD [%]	0.1749	0.1829	0.1825
Nuclear data RSD [%]	NaN	0.2649	0.5232

Another important quantity for the design of ARC is the volumetric power deposited by the neutrons in the main components of the ARC reactor. The results for beryllium and fluorine are shown in tables IV and V, respectively. Again, the results obtained with the two methods are comparable, even if the discrepancy is larger with respect to the TBR results. Moreover, in this case the nuclear data uncertainty depends on the amount of the specific nuclide present in the different components. In fact, the largest uncertainty with fluorine is in the cooling channel (CC) and the breeding blanket (BB), as they are mainly composed of ^{19}F, while for the beryllium the largest contribution is in the neutron multiplier (NM) layer, made of solid ^{9}Be.

TABLE IV
Nuclear data uncertainty of ^{9}Be for the volumetric power deposition using the ENDF-B/VIII.0 library[1].

Fast Total Monte Carlo						
	FW	VV1	CC	NM	VV2	BB
Volumetric power deposition [MW/m^3]	0.911(5)	4.46(1)	10.79(4)	5.55(9)	2.336(6)	0.714(2)
Nuclear data RSD [%]	0.1461	0.1022	0.3292	1.6031	0.1490	0.1604
GRS						
	FW	VV1	CC	NM	VV2	BB
Volumetric power deposition [MW/m^3]	0.906(5)	4.45(1)	10.75(4)	5.51(9)	2.333(6)	0.714(1)
Nuclear data RSD [%]	0.1137	0.1042	0.3248	1.629	0.1884	0.1402

[1] The number in parenthesis is the total uncertainty and has to be intended as ± on the last digit of the result.

An additional analysis has been performed to evaluate the impact of the nuclear uncertainties of ^{58}Ni, which is the main constituent of Inconel-718, i.e. the material composing the structure of the vacuum vessel. Despite the vacuum vessel represents only around 3% of the total volume of ARC, it is possible to see in table VI that the influence of the nuclear data uncertainties of

TABLE V
Nuclear data uncertainty of ^{19}F for the volumetric power deposition using the ENDF-B/VIII.0 library[1,2].

Fast Total Monte Carlo						
	FW	VV1	CC	NM	VV2	BB
Volumetric power deposition [MW/m^3]	0.910(6)	4.45(3)	10.8(2)	5.55(4)	2.34(2)	0.714(6)
Nuclear data RSD [%]	0.4345	0.5200	1.5416	0.6267	0.8198	0.8872
GRS						
	FW	VV1	CC	NM	VV2	BB
Volumetric power deposition [MW/m^3]	0.905(7)	4.44(3)	10.7(2)	5.54(4)	2.33(2)	0.713(7)
Nuclear data RSD [%]	0.5216	0.5481	1.5683	0.6051	0.8244	0.9024

[1] The number in parenthesis is the total uncertainty and has to be intended as ± on the last digit of the result.
[2] FW: first wall; VV1: inner vacuum vessel; CC: cooling channel; NM: neutron multiplier; VV2: outer vacuum vessel; BB: breeding blanket.

this nuclide on responses like the TBR is not only non-negligible, but also more relevant than the other nuclides considered in this work. This aspect highlights the importance of a thorough nuclear data uncertainty propagation study, which should involve all the nuclides present in the reactor components. Since the aim of the paper is to assess the non-intrusive techniques presented in section III on the nuclides constituting the salt, the complete uncertainty propagation study is left as a future development of this activity.

TABLE VI
Nuclear data uncertainty of ^{58}Ni for the TBR and the volumetric power deposition using the ENDF-B/VIII.0 library[1].

Fast Total Monte Carlo						
TBR	1.086±0.008					
Nuclear data RSD [%]	0.6784					
	FW	VV1	CC	NM	VV2	BB
Volumetric power deposition [MW/m^3]	0.911(5)	4.4(2)	10.79(6)	5.55(3)	2.33(9)	0.714(6)
Nuclear data RSD [%]	0.2926	4.624	0.4947	0.4537	3.679	0.9055

[1] The number in parenthesis is the total uncertainty and has to be intended as ± on the last digit of the result.

Finally, in order to establish if the GRS is actually less sensitive to the impact of the statistical noise, we have applied the fTMC and the GRS on ^{6}Li in the case of a simplified version of ARC, in order to speed up the analysis. This simplified model corresponds to a toroidal geometry with exactly the same layers of ARC, a major radius of 3.3 m and a maximum minor radius of

2 m. Both the methods have been applied with 5×10^3 neutron histories per batch, 50 batches per simulation and 1000 simulations. Considering as an example the profile of relative standard deviation associated with the power deposition in the inner vacuum vessel of the simplified model, fig. 9, it is clear that with the GRS the convergence is reached after about 500 simulations, while the fTMC is far from the convergence and it is even possible that it will never reach the convergence. This result justifies the adoption and the usefulness of the GRS, particularly when the effect of the nuclear data uncertainties is small.

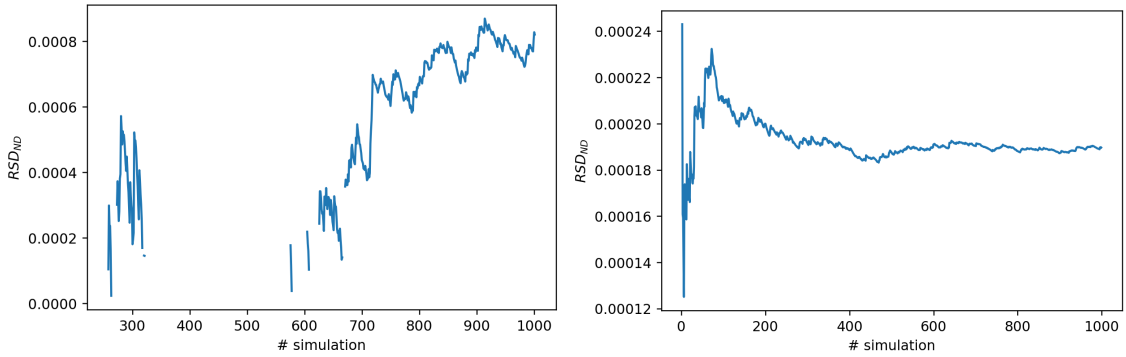

(a) (b)

Fig. 9. Profile of the relative standard deviation of the power deposition in the inner vacuum vessel due to the nuclear data uncertainties of ^{6}Li of the simplified ARC model with (a) fTMC and (b) GRS.

IV.B. Unscented Transform

Concerning the Unscented Transform method, a larger neutron population was considered, in order to further reduce the statistical noise in the output responses. In fact, the fTMC and the GRS were specifically tailored for stochastic models, thus they manage to provide meaningful results even with non-negligible statistical errors. On the contrary, the UT was conceived for deterministic models, thus it should require, theoretically, no statistical noise at all. To reduce the impact of this unavoidable issue featuring the Serpent responses, the total neutron population has been increased to 6×10^6, i.e. 1.2×10^5 neutron histories per batch, leading to a statistical error smaller than 1%.

At first, the UT has been applied to beryllium. Figure 10 shows the covariance matrices of the two most important cross sections of the beryllium, i.e. the elastic scattering (MT=2) and the

radiative capture (MT=102), obtained with SANDY.

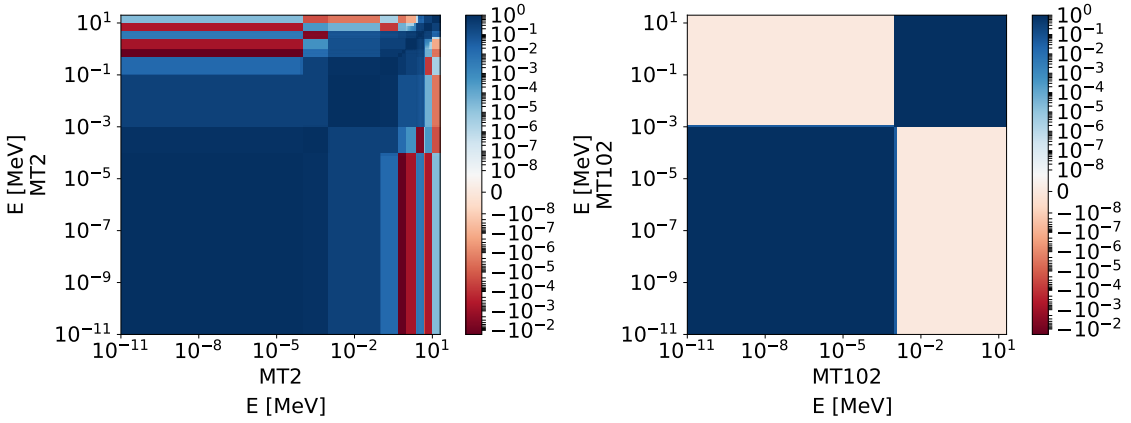

(a) (b)

Fig. 10. Covariance matrices for elastic scattering (a, MT=2) and radiative capture (b, MT=102) for ^{9}Be taken from ENDF-B/VIII.0 library.

The cornerstone of the UT is the generation of a sufficient number of sigma points computed according to eq. (4) in order to approximate the covariance matrices. Using the SVD and truncating at an energy of 99.997%, the resulting covariance matrices obtained using the sigma points are displayed in fig. 11, showing that the pattern of the covariance has been preserved, despite only 40 singular values over 3133 are used.

Moreover, it was also numerically verified that this truncation energy guarantees that the relative difference with respect to the original covariance matrix is smaller than 1%. For these reasons, it is possible to claim that the reduced covariance matrix reconstructed from the sigma points is in good agreement with the original one. The main consequence of this truncation, considering that the reconstructed matrices are similar to the initial ones, is a dramatic reduction of the computational cost (i.e., 81 simulations instead of 6267), which makes the UT approach competitive with the fTMC and GRS methods. It is also possible to observe (fig. 12) that the truncation energy selected is particularly appropriate in the case of ^{9}Be, since it corresponds to a very fast decay in the magnitude of the singular values.

The sigma points and the results for the beryllium (shown in table VII) have been obtained with $\lambda = 0.5$. This choice avoids the presence of negative weights and generates weights featured by the same value. An effect of this feature is that the mean obtained through the UT is exactly the arithmetic mean of the responses of interest. This choice also limits the appearance of negative

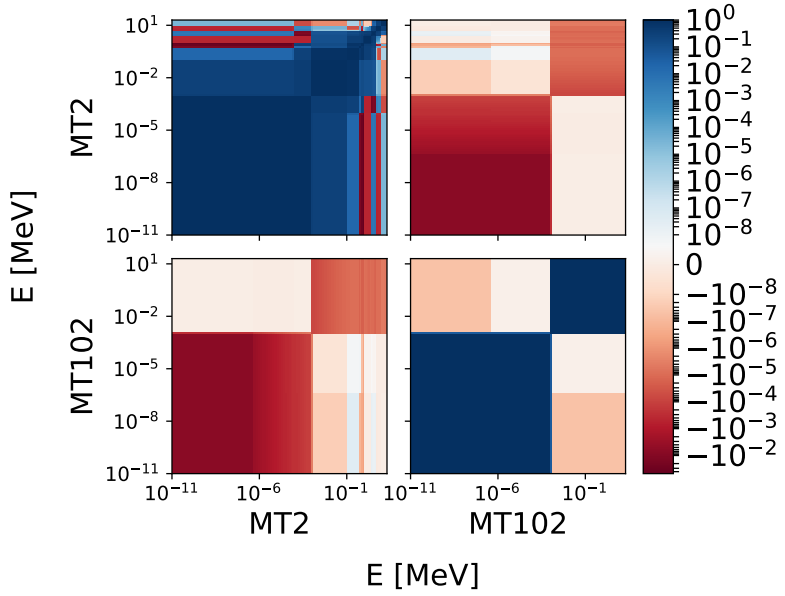

Fig. 11. Covariance matrices for ^{9}Be reconstructed from the sigma points, considering a truncation energy of 99.997%.

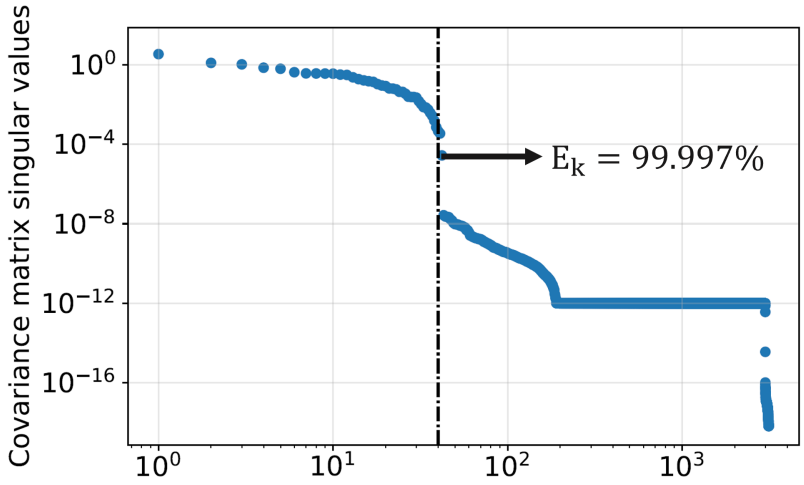

Fig. 12. Magnitude of the 3133 singular values of ^{9}Be nuclear data covariance matrix. The black line corresponds to the truncation energy of 99.997%.

variances, as for the case where $t + \lambda = 3$. Further analyses are currently under way to investigate whether this is a general issue associated with negative λ values for Monte Carlo codes, or if it is due to the fact that, with $\lambda < 0$, the results with Serpent are less spread and, thus, partially blurred by the statistical error (fig. 13). In fact, the standard deviation of the vector of TBRs using $t + \lambda = 3$ is comparable with the difference between two values of TBR obtained with two different

Serpent simulation and using the nominal nuclear data. A possible solution in this sense can be to further increase the number of neutron histories with negative λ. From this point of view, it seems that the fTMC and GRS are advantageous since they are able to deal with larger statistical errors but, on the other hand, they generally require a larger number of Serpent simulations.

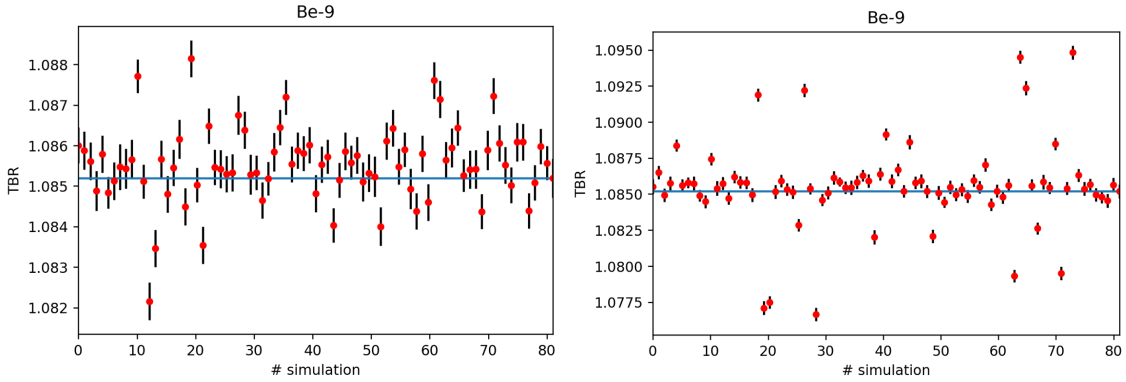

(a) (b)

Fig. 13. Scatter plot of the TBR values resulting from the 81 simulations of the UT method with $t + \lambda = 3$ (a) and with $\lambda = 0.5$. The black lines represent the error bars (1σ).

Another set of simulations was performed with $\lambda = 0$: in this case, the weight associated with the case run with the expected value of the nuclear data is identically 0, i.e. it is taken into account in the UT calculation. The results are comparable with those obtained with $\lambda = 0.5$ and with the fTMC and GRS.

TABLE VII
Nuclear data uncertainty of ^{9}Be with UT for the TBR and the volumetric power deposition using the ENDF-B/VIII.0 library[1].

Unscented Transform						
	FW	VV1	CC	NM	VV2	BB
Volumetric power deposition [MW/m^3]	0.910(1)	4.455(6)	10.79(4)	5.55(9)	2.336(4)	0.714(1)
Nuclear data RSD [%]	0.1574	0.1268	0.3297	1.5916	0.1762	0.1742
TBR	1.086±0.003					
Nuclear data RSD [%]	0.2689					

[1] The number in parenthesis is the total uncertainty and has to be intended as ± on the last digit of the result.

Since one of the outcomes of the fTMC and the GRS analyses is that the influence of the nuclear data uncertainties of ^{19}F is non-negligible, the UT has been performed also on this nuclide, with the same settings used for ^{9}Be. In this case, truncating at an energy of the singular values of

99.997% lead to 100 singular values, which means 201 Serpent simulations. The results obtained with $\lambda = 0.5$ are shown in table VIII: in this case there are non-negligible differences with respect to the fTMC and GRS methods, probably because truncating at 99.997% is not sufficient for the fluorine. In fact, considering the behaviour of the singular values of ^{19}F (fig. 14), it is not possible to observe a sharp decay in the magnitude of the singular values like in the case of beryllium, so it should be necessary to further increase the truncation energy for this nuclide, making the application of the UT more disadvantageous, from the computational point of view, than the adoption of fTMC or GRS. An alternative explanation to this general underestimation with respect to fTMC and GRS results is that some of the sigma points for ^{19}F fall outside the range [0,2], so they are fixed to 0 or 2 by SANDY. This truncation of the sigma points imposed by SANDY limits the magnitude of the largest sigma points and, as a consequence, the variance of the responses of interest.

TABLE VIII
Nuclear data uncertainty of ^{19}F with UT for the TBR and the volumetric power depositionusing the ENDF-B/VIII.0 library[1].

Unscented Transform						
	FW	VV1	CC	NM	VV2	BB
Volumetric power deposition [MW/m^3]	0.911(4)	4.46(2)	10.8(1)	5.55(3)	2.34(2)	0.714(5)
Nuclear data RSD [%]	0.4917	0.5107	1.3746	0.5633	0.7572	0.7636
TBR	1.086±0.005					
Nuclear data RSD [%]	0.4536					

[1] The number in parenthesis is the total uncertainty and has to be intended as ± on the last digit of the result.

IV.C. Polynomial Chaos Expansion

Finally, some results were obtained applying the PCE on ^{9}Be, using the pseudo-spectral method with a quadrature order I=1 and a polynomial expansion order K=1. The choice of using the lowest approximation orders is due to the fact that these parameters lead to the lowest number of Serpent evaluations. With these calculation settings, and considering the reduced covariance matrix, the required number of Serpent simulations was 81. Also in this case, 1.2×10^5 neutron histories per batch and 50 batches were used in order to have a statistical error smaller than 1% for the responses of interest. The results in table IX show a significant difference with respect to the results obtained in the previous sections. The lack of accuracy between the methods can

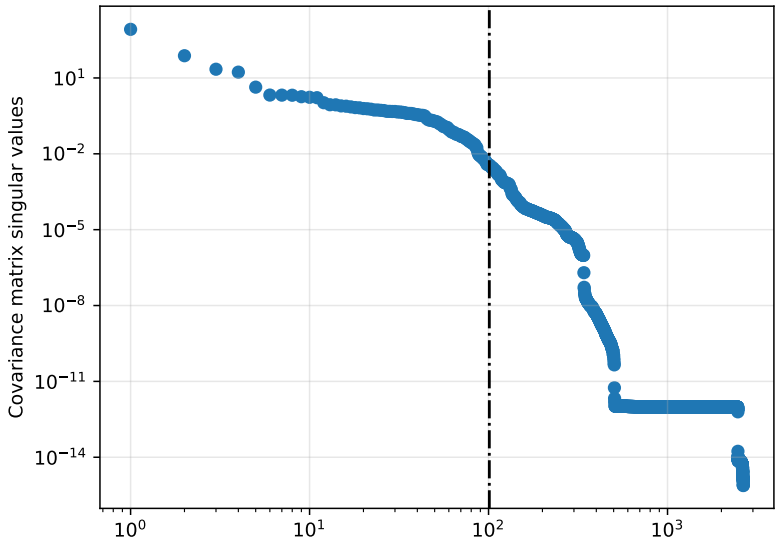

Fig. 14. Magnitude of the 2651 singular values of ^{19}F nuclear data covariance matrix. The black dotted line corresponds to the truncation energy of 99.997%.

be justified by the fact that, to accurately compute the PCE coefficients, I should be equal to $K+1$. However, this is not computationally affordable, because the minimum degree $I=2$ would correspond, in the case of ^{9}Be, to more than 3300 Serpent simulations. With such a large number of independent runs, the application of TMC would definitively be much faster than the PCE method. In light of these considerations, it is possible to conclude that the PCE method is not suited for the uncertainty propagation involving the nuclear data due to their large number of degrees of freedom.

TABLE IX
Nuclear data uncertainty of ^{9}Be with PCE for the TBR and the volumetric power deposition using the ENDF-B/VIII.0 library[1].

Polynomial Chaos Expansion						
	FW	VV1	CC	NM	VV2	BB
Volumetric power deposition [MW/m^3]	0.911(5)	4.45(1)	10.78(3)	5.54(7)	2.336(8)	0.714(2)
Nuclear data RSD [%]	0.6333	0.290	0.309	1.194	0.323	0.222
TBR	1.085±0.003					
Nuclear data RSD [%]	0.2870					

[1] The number in parenthesis is the total uncertainty and has to be intended as ± on the last digit of the result.

IV.D. Impact of the nuclear data library selection

In section II the influence of the choice of the nuclear data library on the responses of interest in the best estimate case has been underlined. Thus, it is important to assess their impact on the results of the uncertainty propagation analysis as well. All the UP methods employed in this work are sampling-based methods which require the evaluation of the nuclear data covariance matrices, making the sample generation process dependent on the library selection.

Some features of the covariances for the isotopes of interest allowed to reduce the number of simulation campaigns. First of all, the covariance matrices of ^{19}F and ^{9}Be from the FENDL-3.2b library are identical to the ones from the ENDF-B/VIII.0 library. Then, the JEFF-3.3 library does not contain information about the covariance matrices of elastic scattering (MT=2) and of neutronic multiplication (MT=16) for ^{9}Be, which are two of the most important reaction channels for ARC. Thus, also this case was avoided. Therefore, considering the impact of ^{19}F, the following analysis focuses on the case in which the nuclear data of this nuclide are perturbed. To highlight the effect of the single covariance on the overall uncertainty of a specific isotope, each calculation is carried out using the reference library for the transport calculation, i.e. ENDF-B/VIII.0, but sampling the perturbed files according to the covariance taken from JEFF-3.3.

In fig. 15 a comparison between the main diagonal values of the covariance matrices for the total cross elastic scattering (MT=2) and radiative capture (MT=102) of ^{19}F with the ENDF-B/VIII.0 and the JEFF-3.3 libraries are presented. According to these graphs, it can be expected that the nuclear data relative standard deviation obtained with the perturbed ACE files generated using JEFF-3.3 would be higher than those perturbed with ENDF-B/VIII.0 (see table II and table V). Indeed, the results obtained through the fTMC show larger values of the nuclear data uncertainties for the TBR, but not for the power deposition (see table X). This is probably due to the fact that in fig. 15 only the values on the main diagonal of the covariance matrix (i.e. the variances) have been taken into account. However, if one considers the whole covariance matrix, it is possible to notice that, in general, JEFF-3.3 misses some covariance values, in particular at higher energies, which are of interest in this work. Figure 16 shows an example of the matrices for the radiative capture (MT=102).

In principle, another possible cause could be related to different values in the covariances of the KERMA coefficients, which directly impact the evaluation of power deposition. However,

since no covariance matrices are available for any nuclear data library, the discrepancy could not be attributed to this aspect.

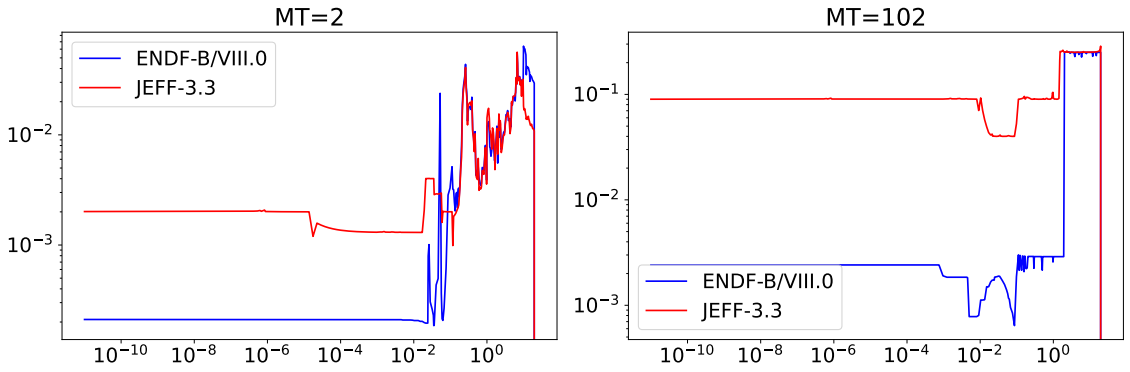

(a) (b)

Fig. 15. Comparison between the diagonal values of the covariance matrices for the elastic scattering (MT=2) and radiative capture (MT=102) of ^{19}F with the ENDF-B/VIII.0 and the JEFF-3.3 libraries.

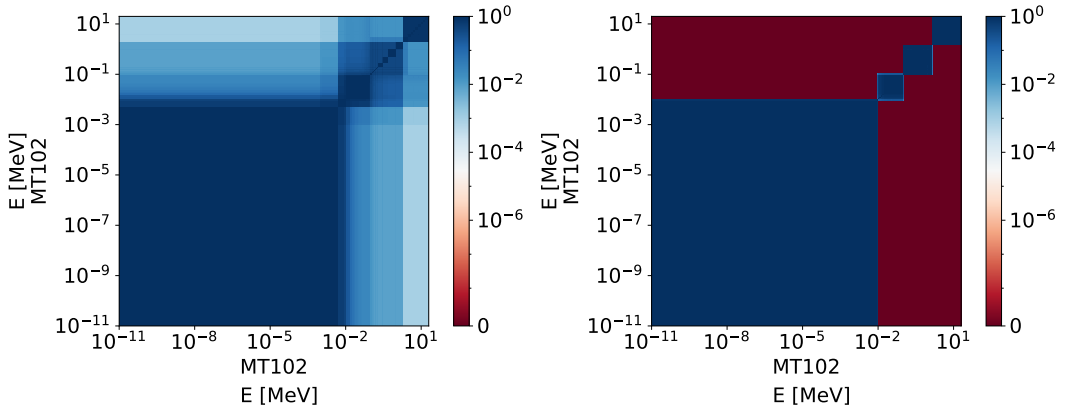

(a) (b)

Fig. 16. Comparison between the covariance matrices for the radiative capture (MT=102) of ^{19}F with the ENDF-B/VIII.0 (a) and the JEFF-3.3 (b) libraries. Many values are missing in the JEFF-3.3 covariance matrix for energies larger than 0.01 MeV

Since the library used for the unperturbed nuclides is always the same for the various calculations, i.e. ENDF-B/VIII.0, the mean values of the responses of interest are similar (see table X), as it could be reasonably expected.

To take into account the effect of changing the library for the transport calculations, a second set of simulations consisted in the adoption of the JEFF-3.3 and of the FENDL-3.2b libraries for

TABLE X
Nuclear data uncertainty of ^{19}F for the TBR and the volumetric power deposition evaluated with the fast Total Monte Carlo method using different libraries[1].

ENDF-B/VIII.0+JEFF-3.3 (for covariances)						
	FW	VV1	CC	NM	VV2	BB
Volumetric power deposition [MW/m^3]	0.911(6)	4.45(2)	10.8(1)	5.54(4)	2.33(2)	0.714(5)
Nuclear data RSD [%]	0.3432	0.3735	1.2226	0.5879	0.7771	0.6824
TBR			1.085±0.008			
Nuclear data RSD [%]			0.7270			
JEFF-3.3						
	FW	VV1	CC	NM	VV2	BB
Volumetric power deposition [MW/m^3]	0.20(2)	4.72(2)	10.8(1)	5.86(4)	2.48(2)	0.715(5)
Nuclear data RSD [%]	1.989	0.3611	1.186	0.6327	0.7771	0.6790
TBR			1.085±0.008			
Nuclear data RSD [%]			0.7266			
ENDF-B/VIII.0						
	FW	VV1	CC	NM	VV2	BB
Volumetric power deposition [MW/m^3]	0.910(6)	4.45(3)	10.8(2)	5.55(4)	2.34(2)	0.714(6)
Nuclear data RSD [%]	0.4345	0.5200	1.5416	0.6267	0.8198	0.8872
TBR			1.086±0.006			
Nuclear data RSD [%]			0.5245			

[1] The number in parenthesis is the total uncertainty and has to be intended as ± on the last digit of the result.

both the unperturbed and the perturbed nuclides. For the reason discussed previously, it was not possible to study the case of ^{9}Be with JEFF-3.3. During this analysis, it was noticed that FENDL-3.2b contains far less covariance matrices and far less significant reaction channels for ^{19}F than ENDF-B/VIII.0 and JEFF-3.3. Thus, the case of FENDL-3.2b was investigated both for the unperturbed nuclides and for the perturbation of ^{9}Be, while the case of JEFF-3.3 was analysed both for the unperturbed nuclides and for the perturbation of ^{19}F.

As expected, the nuclear data uncertainties obtained in the case of JEFF-3.3 for ^{19}F (table X) are similar to the ones obtained using ENDF-B/VIII.0 for the unperturbed nuclides and JEFF-3.3 to perturb ^{19}F (table X), since the covariance matrices are the same.

As one could expect, the best estimate values are different since the JEFF-3.3 library was used instead of the reference ENDF-B/VIII.0. Also in the case of FENDL-3.2b for ^{9}Be, the nuclear data uncertainties (table XI) are similar to the ones shown in table II and table IV, since the covariance matrices of FENDL-3.2b are the same of ENDF-B/VIII.0 for what concerns ^{9}Be.

TABLE XI
Nuclear data uncertainty of ^{9}Be for the TBR and the volumetric power deposition evaluated with the fast Total Monte Carlo method using different libraries[1].

FENDL-3.2						
	FW	VV1	CC	NM	VV2	BB
Volumetric power deposition [MW/m^3]	0.906(4)	4.68(1)	10.72(4)	5.63(8)	2.452(6)	0.715(1)
Nuclear data RSD [%]	0.0608	0.1065	0.3509	1.5642	0.1726	0.1530
TBR			1.072±0.003			
Nuclear data RSD [%]			0.2743			
ENDF-B/VIII.0						
	FW	VV1	CC	NM	VV2	BB
Volumetric power deposition [MW/m^3]	0.911(5)	4.46(1)	10.79(4)	5.55(9)	2.336(6)	0.714(2)
Nuclear data RSD [%]	0.1461	0.1022	0.3292	1.6031	0.1490	0.1604
TBR			1.086±0.003			
Nuclear data RSD [%]			0.2631			

[1] The number in parenthesis is the total uncertainty and has to be intended as ± on the last digit of the result.

IV.E. Impact of the different energy group structures

So far, all the results presented in this work have been obtained scoring the covariances using the CSWEG-239 group structure.[37] This is the default structure used in SANDY and it consists of a fine grid in the fast range and of an extremely coarse subdivision for $E < 10^{-6}$MeV, which is consistent with the fast neutron spectrum of ARC. However, using a grid with such a large number of energy groups, combined with a large number of reaction channels, leads to pretty larger covariance matrices. The dimension of the covariance matrix can be reduced employing the SVD, as explained in section III.C, and thanks to this operation it was possible to adopt the CSWEG-239 group structure also in the UT method.

However, operating on a smaller covariance matrix could generate an even smaller number of singular values and, thus, of Serpent simulations after the reduction through the SVD. For this reason, the UT approach was applied to the case of ^{9}Be using the ECCO-33 group structure,[38] with the aim of checking if it could lead to results similar to the CSWEG-239 but with less Serpent simulations.

With a truncation energy of 99.997%, only 25 singular values are retained, for a total of 51 Serpent simulations required to evaluate the nuclear data relative standard deviation. This choice induces a reduction of approximately a factor of 1.6 in the simulation time with respect to the

CSWEG-239 (considering, again, 6×10^6 neutron histories and λ=0.5). Concerning the results (table XII), the mean values and the nuclear data RSDs are similar to the ones obtained with 240 groups. This means that, at least for ^{9}Be, the best choice turns out to be selecting the energy group structure ECCO-33, since it allows to reduce the computational cost with the same level of accuracy of the finer case.

In fig. 17, it can be observed that also in this case the truncation energy of 99.997% corresponds to a sudden drop in the magnitude of the singular values. Since using the ECCO-33 the number of Serpent simulations is reduced, the SVD energy was increased so that the truncation error occurs in correspondence of the start of a *plateau* in fig. 17 (i.e. 50 singular values), in order to observe if, with an energy of 99.997%, some information about the covariance matrix is lost. The results obtained (table XIII) show that the difference between the two truncation energy is negligible, confirming that 99.997% is a good value for ^{9}Be

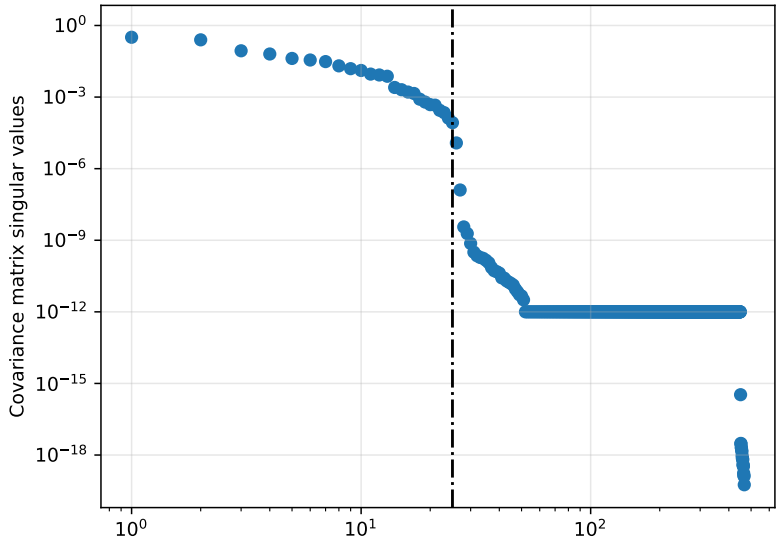

Fig. 17. Magnitude of the 468 singular values of ^{9}Be nuclear data covariance matrix using the ECCO-33. The black line corresponds to the truncation energy of 99.997%.

Thanks to the fact that with ^{9}Be it was possible to show that the ECCO-33 gives results similar to the CSWEG-239, we also tried to employ that energy group structure even for ^{19}F. This case is even more interesting if one considers that, using the ECCO-33 and a truncation energy of 99.997%, the cut is in proximity of a drop in the singular values plot (see fig. 18), differently from what occurred with the CSWEG-239 (see fig. 14). Now, the number of singular values is 51 and

TABLE XII
Nuclear data uncertainty of ^{9}Be with UT, 33 energy groups and 25 singular values for the TBR and the volumetric power deposition using the ENDF-B/VIII.0 library[1].

Unscented Transform						
	FW	VV1	CC	NM	VV2	BB
Volumetric power deposition [MW/m^3]	0.910(2)	4.455(6)	10.79(4)	5.55(9)	2.336(4)	0.714(1)
Nuclear data RSD [%]	0.1975	0.1307	0.3393	1.604	0.1731	0.1793
TBR	1.086±0.003					
Nuclear data RSD [%]	0.2796					

[1] The number in parenthesis is the total uncertainty and has to be intended as ± on the last digit of the result.

TABLE XIII
Nuclear data uncertainty of ^{9}Be with UT, 33 energy groups and 50 singular values for the TBR and the volumetric power deposition using the ENDF-B/VIII.0 library[1].

Unscented Transform						
	FW	VV1	CC	NM	VV2	BB
Volumetric power deposition [MW/m^3]	0.910(2)	4.455(6)	10.79(3)	5.55(9)	2.336(4)	0.714(1)
Nuclear data RSD [%]	0.1684	0.1290	0.3220	1.5885	0.1781	0.1721
TBR	1.086±0.003					
Nuclear data RSD [%]	0.2769					

[1] The number in parenthesis is the total uncertainty and has to be intended as ± on the last digit of the result.

the number of Serpent simulation 103.

Actually, the results in table XIV show that there is a non negligible difference with respect to the results obtained with the fTMC and 240 energy groups (table V), which are considered the reference ones. This is probably due to the fact that the ECCO-33 is not sufficient in the case of ^{19}F, differently from ^{9}Be.

TABLE XIV
Nuclear data uncertainty of ^{19}F with UT and 33 energy groups for the TBR and the volumetric power deposition. using the ENDF-B/VIII.0 library[1].

Unscented Transform						
	FW	VV1	CC	NM	VV2	BB
Volumetric power deposition [MW/m^3]	0.910(4)	4.46(2)	10.8(1)	5.55(3)	2.34(1)	0.714(5)
Nuclear data RSD [%]	0.4279	0.4617	1.3223	0.5766	0.7874	0.8007
TBR	1.086±0.004					
Nuclear data RSD [%]	0.3802					

[1] The number in parenthesis is the total uncertainty and has to be intended as ± on the last digit of the result.

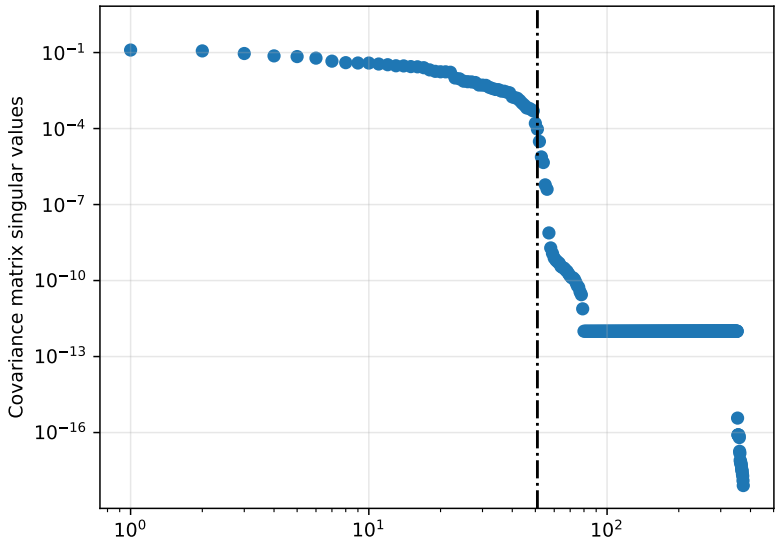

Fig. 18. Magnitude of the 374 singular values of ^{19}F nuclear data covariance matrix using the ECCO-33. The black line corresponds to the truncation energy of 99.997%.

Another set of simulations has been performed applying the fTMC to ^{19}F using the ECCO-33, in order to check if the results obtained with this technique are similar to the ones from the UT and 33 energy groups (table XIV), since the energy group structure is the same. It is important to underline that, in the case of the fTMC, the use of the ECCO-33 does not lead to a reduction of the computational time, since 500 Serpent simulations are still required in order to achieve the statistical convergence. As displayed in table XV, there is a good agreement for what concerns the nuclear data RSDs for the power deposition in the different components of ARC. However, the result for the TBR is larger and more similar to the one evaluated with the fTMC and 240 energy groups (table II). Further investigations will try to explain the reasons of this discrepancy.

Finally, we have made also an attempt applying the PCE to ^{9}Be using the ECCO-33, in order to see if the reduction of the energy structure was sufficient to significantly reduce the number of simulations required and make the application of the PCE feasible too. Actually, the reduction was important, passing from 3321 simulations with CSWEG-239 to 1326 with ECCO-33. However, this reduction is still not sufficient to justify the use of the PCE for this type of problem in place of the TMC.

TABLE XV
Nuclear data uncertainty of ^{19}F with fTMC and 33 energy groups for the TBR and the volumetric power deposition using the ENDF-B/VIII.0 library[1].

Unscented Transform						
	FW	VV1	CC	NM	VV2	BB
Volumetric power deposition [MW/m^3]	0.911(6)	4.46(2)	10.8(1)	5.55(4)	2.34(2)	0.715(6)
Nuclear data RSD [%]	0.4223	0.4412	1.3349	0.6077	0.7764	0.7924
TBR	1.086±0.006					
Nuclear data RSD [%]	0.5306					

[1] The number in parenthesis is the total uncertainty and has to be intended as ± on the last digit of the result.

V. CONCLUSIONS

The results of the uncertainty propagation analysis in the ARC reactor obtained with three methods employed in this work (fast Total Monte Carlo, GRS and Unscented Transform) are comparable in terms of nuclear data relative standard deviation. From the point of view of the computational time, the UT is comparable to fTMC and GRS when the number of singular values necessary to reproduce the covariance matrix is smaller than the number of simulation required for the fTMC and the GRS (generally larger than 500), as in the case of beryllium. For other nuclides, like fluorine and fissile elements, featured by many resonances, it is expected that the UT is not the most suitable choice.

Table XVI shows the total computational time for ^{9}Be and ^{19}F using the ENDF-B/VIII.0 library. The fTMC seems the fastest method, but its computational cost does not depend on the energy structure employed. On the other hand, the computational time of the UT decreases if the number of energy groups is smaller, however it remains larger than the fTMC, specially for heavier nuclides. This is mainly due to the fact that the number of neutron histories in the UT has been increased with respect to the fTMC in order to reduce the statistical error. If one finds the optimum number of neutron histories, it is possible that the UT will lead to a smaller computational time than the fTMC. Concerning GRS, its computational time is larger because in this work it has been applied through a number of Serpent simulations double than the number adopted for fTMC. However, as explained in section IV.A, in principle GRS leads to a converged result in a smaller number of Serpent simulations (i.e. in a smaller computational time) than fTMC, especially when the nuclear data uncertainties are small. In the future, the application of

deterministic perturbation-based sensitivity/uncertainty techniques would possibly help in further increasing the computational efficiency of the uncertainty propagation in ARC.

TABLE XVI
Total number of CPU-hours for the three methods employed in this work with both the CSWEG-239 and the ECCO-33 energy grid structures.

CSWEG-239		
	^{9}Be	^{19}F
Fast Total Monte Carlo [h]	533	533
GRS [h]	1066	1066
Unscented Transform [h]	1210	3002
ECCO-33		
	^{9}Be	^{19}F
Fast Total Monte Carlo [h]	-	533
GRS [h]	-	-
Unscented Transform [h]	762	1538

The resultsof the UP show that the contribution of each specific nuclide is not sufficient to reduce the TBR of ARC below one. However, it is possible that the combination of the nuclear data uncertainties of all the nuclides present in ARC could lead to a TBR smaller than one.

The PCE approach appears not feasible for the nuclear data uncertainty propagation where the dimensionality of the problem is huge, even after a reduction of the dimension of the problem. However, it will be interesting to apply the PCE to similar problems, like a multi-group model where the dimension of the problem is expected to be smaller, since the PCE will allow us to evaluate not only the mean and the variance of the responses of interest, but also their distribution.

For what concerns the nuclear data library selection, the responses of interest for this work significantly changed according to the library used, namely ENDF-B/VIII.0, JEFF-3.3 and FENDL-3.2b. In particular, FENDL-3.2b resulted in a smaller TBR than the other libraries; thus, in order to have a conservative design, it should be better to use FENDL-3.2b for the neutronic evaluations. Some covariance matrices of ^{19}F are missing in the FENDL-3.2b library so, in the case of an uncertainty propagation study, the suggestion is to use ENDF-B/VIII.0 for the perturbation of the nuclear data and FENDL-3.2b for the nominal data.

The impact of different energy grids on the UP has been considered too. The use of coarser energy grids like the ECCO-33 can be a significant improvement in the case of methods like the UT, since it allows to reduce the required number of Monte Carlo simulations. However, in the case of

heavier nuclides, coarser grids give different results, probably because of the poorer representation of cross sections. Thus, the selection of the UP method and of the energy grid strongly depends on the nuclide that is taken into account.

Finally, in this work, we focused on integral quantities like the TBR and the average neutron power deposition, which are in general affected by smaller statistical errors. On the other hand, if one is interested in the UP of localized responses for this class of fixed-source problems, where the parameters of interest may have larger statistical uncertainties, the use of variance reduction methods can lead to a further computational cost saving, if combined to the methods described in this work.

Table XVII and table XVIII summarise the nuclear data RSD of the nuclides studied in this work and the sum of their contribution to the TBR and to the total neutron power deposited in ARC, respectively.

TABLE XVII
Nuclear data RSD of ^{6}Li, ^{9}Be and ^{19}F computed with the three methods employed in this work and the CSWEG-239 for the TBR and their total contribution to the TBR uncertainty.

ENDF-B/VIII.0					
	^{6}Li	^{9}Be	^{19}F	Total	TBR
fTMC	0.0135%	0.2631%	0.5245%	0.5869%	1.086±0.006
GRS	-	0.2649%	0.5232%	0.5865%	1.085±0.006
UT	-	0.2689%	0.4730%	0.5441%	1.086±0.006
ENDF-B/VIII.0+JEFF-3.3 (for covariances)					
	^{6}Li	^{9}Be	^{19}F	Total	TBR
fTMC	-	-	0.7270%	0.7270%	1.085±0.008
JEFF-3.3					
	^{6}Li	^{9}Be	^{19}F	Total	TBR
fTMC	-	-	0.7266%	0.7266%	1.085±0.008
FENDL-3.2					
	^{6}Li	^{9}Be	^{19}F	Total	TBR
fTMC	-	0.2631%	-	0.2631%	1.072±0.003

ACKNOWLEDGMENTS

Computational resources were provided by HPC@POLITO, a project of Academic Computing within the Department of Control and Computer Engineering at Politecnico di Torino

TABLE XVIII
Nuclear data RSD of ^{6}Li, ^{9}Be and ^{19}F computed with the three methods employed in this work and the CSWEG-239 for the total neutron power deposition and their total contribution to the total neutron power deposition uncertainty.

ENDF-B/VIII.0					
	^{6}Li	^{9}Be	^{19}F	Total	Power
fTMC	0.0535%	0.1483%	0.4092%	0.4385%	345.33±0.02 MW
GRS	0.0315%	0.1515%	0.4112%	0.4393%	345.13±0.02 MW
UT	-	0.1507%	0.3612%	0.3914%	345.28±0.01 MW
ENDF-B/VIII.0+JEFF-3.3 (for covariances)					
	^{6}Li	^{9}Be	^{19}F	Total	Power
fTMC	-	-	0.3324%	0.3324%	345.20±0.01 MW
JEFF-3.3					
	^{6}Li	^{9}Be	^{19}F	Total	Power
fTMC	-	-	0.3357%	0.3357%	349.06±0.01 MW
FENDL-3.2					
	^{6}Li	^{9}Be	^{19}F	Total	Power
fTMC	-	0.1479%	-	0.1479%	347.598±0.005 MW

(http://www.hpc.polito.it).

The authors would also like to thank Dr. Dimitri Rochman and Dr. Arjan Koning for their kindness and for their precious guidance in the use of the fast Total Monte Carlo method.

REFERENCES

[1] B. Sorbom, J. Ball, T. Palmer, F. Mangiarotti, J. Sierchio, P. Bonoli, C. Kasten, D. Sutherland, H. Barnard, C. Haakonsen, J. Goh, C. Sung, and D. Whyte, "ARC: A compact, high-field, fusion nuclear science facility and demonstration power plant with demountable magnets," *Fusion Engineering and Design*, **100**, 378 (2015).

[2] A. J. H. Donné, W. Morris, X. Litaudon, C. Hidalgo, D. McDonald, H. Zohm, E. Diegele, A. Möslang, K. H. Nordlund, G. Federici, P. Sonato, C. Waldon, D. Borba, and P. Helander, *European Research Roadmap to the Realisation of Fusion Energy*, EUROfusion Consortium, Germany (2018).

[3] J. Leppänen, M. Pusa, T. Viitanen, V. Valtavirta, and T. Kaltiaisenaho, "The

Serpent Monte Carlo code: Status, development and applications in 2013," *Annals of Nuclear Energy*, **82**, 142 (2013).

[4] A. Aimetta, N. Abrate, S. Dulla, and A. Froio, "Neutronic analysis of the fusion reactor ARC: Monte Carlo simulations with the Serpent," *Fusion Science and Technology*, **78**, 275 (2022).

[5] A. Aimetta, "Neutronic analysis of the fusion reactor ARC: Monte Carlo simulations with the Serpent code," (2020); 10.5281/zenodo.5118690., URL https://doi.org/10.5281/zenodo.5118690.

[6] D. G. Cacuci, *Sensitivity & Uncertainty Analysis, Volume I: Theory*, Chapman & Hall/CRC, New York (2003); 10.1201/9780203911396.ch10.

[7] A. Gandini, M. Salvatores, and I. D. Bono, "Sensitivity Study of Fast Reactors Using Generalized Perturbation Techniques," *Fast Reactor Physics Vol. I. Proceedings of a Symposium on Fast Reactor Physics and Related Safety Problems* (1968).

[8] M. Aufiero, M. Martin, and M. Fratoni, "XGPT: Extending Monte Carlo Generalized Perturbation Theory capabilities to continuous-energy sensitivity functions," *Annals of Nuclear Energy*, **96**, 295–306 (2016).

[9] Abrate, N., Aufiero, M., Dulla, S., and Fiorito, L., "Nuclear data uncertainty quantification in molten salt reactors with XGPT," *International Conference on Mathematics Computational Methods and Reactor Physics* (2019).

[10] N. Abrate, S. Dulla, and P. Ravetto, "Generalized perturbation techniques for uncertainty quantification in lead-cooled fast reactors," *Annals of Nuclear Energy*, **164**, 108623 (2021); https://doi.org/10.1016/j.anucene.2021.108623., URL https://www.sciencedirect.com/science/article/pii/S0306454921004990.

[11] A. Koning and D. Rochman, "Towards sustainable nuclear energy: Putting nuclear physics to work," *Annals of Nuclear Energy*, **35**, 2024 (2008); https://doi.org/10.1016/j.anucene.2008.06.004., URL https://www.sciencedirect.com/science/article/pii/S0306454908001813.

[12] D. Rochman, S. van der Marck, A. Koning, H. Sjöstrand, and W. Zwermann, "Uncertainty Propagation with Fast Monte Carlo Techniques," *Nuclear Data Sheets*, **118**, 367 (2014).

[13] W. Zwermann, B. Krzykacz-Hausmann, L. Gallner, M. Klein, A. Pautz, and K. Velkov, "Aleatoric and epistemic uncertainties in sampling based nuclear data uncertainty and sensitivity analyses," (2012)Proc. of the International Topical Meeting on Advances in Reactor Physics (PHYSOR '12), Knoxville, TN, USA, April 15–20, 2012, on CD-ROM.

[14] S. J. Julier and J. K. Uhlmann, "New extension of the Kalman filter to nonlinear systems," I. Kadar (Editor), *Signal Processing, Sensor Fusion, and Target Recognition VI*, vol. 3068, 182 – 193, International Society for Optics and Photonics, SPIE (1997).

[15] Le Maître O.P. and Knio O.M., *Spectral Methods for Uncertainty Quantification: With Applications to Computational Fluid Dynamics. Scientific Computation*, Springer, Dordrecht (2010).

[16] D. Leichtle, U. Fischer, I. Kodeli, R. Perel, A. Klix, P. Batistoni, and R. Villari, "Sensitivity and uncertainty analyses of the HCLL mock-up experiment," *Fusion Engineering and Design*, **85**, *10*, 1724 (2010); https://doi.org/10.1016/j.fusengdes.2010.05.023., URL https://www.sciencedirect.com/science/article/pii/S0920379610002358, proceedings of the Ninth International Symposium on Fusion Nuclear Technology.

[17] D. Leichtle, U. Fischer, I. Kodeli, R. Perel, M. Angelone, P. Batistoni, P. Carconi, M. Pillon, I. Schäfer, K. Seidel, R. Villari, and G. Zappa, "Sensitivity and uncertainty analyses of the tritium production in the HCPB breeder blanket mock-up experiment," *Fusion Engineering and Design*, **82**, *15*, 2406 (2007); https://doi.org/10.1016/j.fusengdes.2007.08.007., URL https://www.sciencedirect.com/science/article/pii/S0920379607004115, proceedings of the 24th Symposium on Fusion Technology.

[18] U. Fischer, D. Leichtle, and R. Perel, "Monte Carlo based sensitivity and uncertainty analysis of the HCPB Test Blanket Module in ITER," *Fusion Engineering and Design*, **83**, *7*, 1222 (2008); https://doi.org/10.1016/j.fusengdes.2008.06.053., URL https:

//www.sciencedirect.com/science/article/pii/S0920379608001737, proceedings of the Eight International Symposium of Fusion Nuclear Technology.

[19] I. Kodeli, "Multidimensional Deterministic Nuclear Data Sensitivity and Uncertainty Code System: Method and Application," *Nuclear Science and Engineering*, **138**, *1*, 45 (2001); 10.13182/NSE00-43., URL https://doi.org/10.13182/NSE00-43.

[20] B. Kos, A. Čufar, and I. A. Kodeli, "ASUSD nuclear data sensitivity and uncertainty program package: Validation on fusion and fission benchmark experiments," *Nuclear Engineering and Technology*, **53**, *7*, 2151 (2021); https://doi.org/10.1016/j.net.2021.01.034., URL https://www.sciencedirect.com/science/article/pii/S1738573321000553.

[21] A. Bucalossi, A. Petruzzi, M. Kristof, and F. D'Auria, "Comparison between Best-Estimate–Plus–Uncertainty Methods and Conservative Tools for Nuclear Power Plant Licensing," *Nuclear Technology*, **172**, *1*, 29 (2010)URL https://doi.org/10.13182/NT172-29.

[22] F. D'Auria, C. Camargo, and O. Mazzantini, "The Best Estimate Plus Uncertainty (BEPU) approach in licensing of current nuclear reactors," *Nuclear Engineering and Design*, **248**, 317 (2012); https://doi.org/10.1016/j.nucengdes.2012.04.002., URL http://www.sciencedirect.com/science/article/pii/S0029549312001872.

[23] R. Macfarlane, D. W. Muir, R. M. Boicourt, A. C. Kahler, III, and J. L. Conlin, "The NJOY Nuclear Data Processing System, Version 2016," (2017); 10.2172/1338791., URL https://www.osti.gov/biblio/1338791.

[24] U. Fischer, L. Boccaccini, F. Cismondi, M. Coleman, C. Day, Y. Hörstensmeyer, F. Moro, and P. Pereslavtsev, "Required, achievable and target TBR for the European DEMO," *Fusion Engineering and Design*, **155**, 111553 (2020); https://doi.org/10.1016/j.fusengdes.2020.111553., URL https://www.sciencedirect.com/science/article/pii/S0920379620301010.

[25] L. Fiorito, G. Žerovnik, A. Stankovskiy, G. Van den Eynde, and P. Labeau, "Nuclear data uncertainty propagation to integral responses using SANDY," *Annals of Nuclear Energy*, **101**, 359 (2017); https://doi.org/10.1016/j.anucene.2016.11.026., URL https://www.sciencedirect.com/science/article/pii/S0306454916305278.

[26] C. De Mulatier, E. Dumonteil, A. Rosso, and A. Zoia, "The critical catastrophe revisited," *Journal of Statistical Mechanics: Theory and Experiment*, **2015**, *8*, P08021 (2015)URL https://iopscience.iop.org/article/10.1088/1742-5468/2015/08/P08021/meta.

[27] B. Foad, A. Yamamoto, and T. Endo, "Efficient uncertainty quantification for PWR during LOCA using unscented transform with singular value decomposition," *Annals of Nuclear Energy*, **141**, 107341 (2020).

[28] S. Seabold and J. Perktold, "statsmodels: Econometric and statistical modeling with python," *9th Python in Science Conference* (2010).

[29] R. Borsdorf, N. J. Higham, and M. Raydan, "Computing a Nearest Correlation Matrix with Factor Structure," *SIAM Journal on Matrix Analysis and Applications*, **31**, 2603 (2010)URL https://doi.org/10.1137/090776718.

[30] N. Wiener, "The homogeneous chaos," *American Journal of Mathematics*, **60**, *4*, 897 (1938)URL https://doi.org/10.2307/2371268.

[31] D. Xiu and G. E. Karniadakis, "The Wiener–Askey polynomial chaos for stochastic differential equations," *SIAM journal on scientific computing*, **24**, *2*, 619 (2002)URL https://doi.org/10.1137/S1064827501387826.

[32] C. Canuto, M. Y. Hussaini, A. Quarteroni, and T. A. Zang, *Spectral methods: evolution to complex geometries and applications to fluid dynamics*, Springer Science & Business Media (2007)URL https://link.springer.com/book/10.1007/978-3-540-30728-0.

[33] A. Kaintura, T. Dhaene, and D. Spina, "Review of polynomial chaos-based methods for uncertainty quantification in modern integrated circuits," *Electronics*, **7**, *3*, 30 (2018)URL https://doi.org/10.3390/electronics7030030.

[34] R. Bellman, *Dynamic Programming*, Rand Corporation research study, Princeton University Press (1957)URL https://books.google.it/books?id=wdtoPwAACAAJ.

[35] J. Feinberg and H. P. Langtangen, "Chaospy: An open source tool for designing methods of uncertainty quantification," *Journal of Computational Science*, **11**, 46 (2015); https://doi.org/10.1016/j.jocs.2015.08.008., URL https://www.sciencedirect.com/science/article/pii/S1877750315300119.

[36] A. Aimetta, "A non-intrusive nuclear data uncertainty propagation study for the ARC fusion reactor design," (2022); 10.5281/zenodo.7341480., URL https://doi.org/10.5281/zenodo.7341480.

[37] "Cross Section Evaluation Working Group (CSEWG)," URL https://www.nndc.bnl.gov/csewg/.

[38] G. Rimpault, D. Plisson, J. Tommasi, R. Jacqmin, and J. Rieunier, "The ERANOS code and data system for fast reactor neutronic analyses," *International Conference on Physics of Reactors, PHYSOR 2002, Seoul, South Korea*, 1134–1143 (2002)URL https://hal.archives-ouvertes.fr/cea-02906396/.

LIST OF FIGURES

LIST OF TABLES